

# Laser-driven search of axion-like particles including vacuum polarization effects

S. Villalba-Chávez

*Institut für Theoretische Physik I, Heinrich Heine Universität Düsseldorf  
Universitätsstr. 1, 40225 Düsseldorf, Germany*

---

## Abstract

Oscillations of photons into axion-like particles in a high-intensity laser field are investigated. Nonlinear QED effects are considered through the low energy behavior of the vacuum polarization tensor, which is derived from the Euler-Heisenberg Lagrangian in the one-loop and weak field approximations. The expressions obtained in this framework are applied to the configuration in which the strong background field is a circularly polarized monochromatic plane wave. The outcomes of this analysis reveal that, in the regime of low energy-momentum transfer, the axion field induces a chiral-like birefringence and dichroism in the vacuum which is not manifest in a pure QED context. The corresponding ellipticity and angular rotation of the polarization plane are also determined. We take advantage of such observables to impose exclusion limits on the axion parameters. Our predictions cover axion masses for which a setup based on dipole magnets provides less stringent constraints. Possible experimental scenarios in which our results could be tested are also discussed.

*Keywords:* Beyond Standard Model, Vacuum Polarization, Laser Fields, Axion-like particles.

*PACS:* 12.20.-Fv, 14.80.-j

---

## 1. Introduction

The nonlinear vacuum of Quantum Electrodynamics (QED) is an illuminating laboratory for exploring physics beyond the framework of the Standard Model (SM) of fundamental interactions. Over the last few years there have been substantial efforts devoted to employ its unconventional properties in the search of a plausible but elusive pseudo-scalar particle known as the axion. This hypothetical Nambu-Goldstone boson emerges from the spontaneous breaking of the Peccei-Quinn symmetry and turns out to be a distinctive quantity within the solution to the strong CP problem [1, 2, 3]. It additionally conforms to the paradigm of axion-like particles (ALPs) closely associated with some extensions of the SM which naturally emerge from string compactifications [4, 5]. Conceptually the ALPs encompass both scalar and pseudo-scalar bosons [6, 7, 8] being likely candidates for the dark matter of the universe [9, 10, 11, 12]. Their conversion into an electromagnetic field is a long-standing prediction which has been frequently analyzed in a constant magnetic field [13, 14, 15, 16]. In this external field configuration the absorption of a photon into a real ALP induces an attenuation of a probe laser beam. Since the amount of absorbed photons is different for each propagating mode the vacuum behaves as a dichroic medium. Simultaneously, in the presence of an external magnetic field, the ALP-photon coupling modifies the vacuum birefringence caused by the polarization of virtual electron-positron pairs [17, 18, 19, 20]. Both phenomena have inspired polarimetric experiments in which indirect evidence of ALPs could be detected. Among the most significant collaborations are BFRT [21], PVLAS [22], BMV [23] and Q&A [24]. On the other hand, there exists another interesting mechanism of finding traces of the ALPs existence which relies on the photon regenerative property, commonly known as “Light Shining Through a Wall” [25, 26, 27, 28]. This has been experimentally implemented in several collaborations such as ALPS [29, 30], GammeV [31, 32], LIPSS [33], OSQAR [34] and BMV [35, 36]. However, despite the push to detect these particles, the results provided by both kinds of experiments are far from proving that the photon oscillations into ALPs occur. Instead, upper bounds on the

---

*Email address:* selym@tp1.uni-duesseldorf.de (S. Villalba-Chávez)

unknown parameter of ALPs, i.e., coupling constant  $g$  and mass  $m$  have been established, as well as for other weakly interacting particles including paraphotons [37, 38, 39, 40, 41] and mini-charged particles [42, 43, 44, 45, 46, 47]. The main difficulty in these experiments stems from the projected lightness of the ALPs and the weakness of their coupling constants, hence the detection of their tiny observable effects represents a huge technical challenge.

An optimal setup is necessary to overcome this obstacle. Very often the magnetic field strength  $|\mathbf{B}|$  as well as its spatial extension  $\ell$  is exploited to partially achieve this goal. Their combined effects, usually evaluated through the product  $|\mathbf{B}|\ell$ , facilitate the enhancement of observables associated with the mixing process as long as both quantities are increased. Frequently, in high-precision optical experiments, field strengths of the order of  $|\mathbf{B}| \sim \mathcal{O}(10^4 - 10^5)$  G are extended over lengths  $\ell \sim \mathcal{O}(10^2 - 10^3)$  cm so that  $|\mathbf{B}|\ell \sim \mathcal{O}(10^6 - 10^8)$  Gcm. Although the incorporation of interferometric techniques has allowed to extend the interaction region up to macroscopically distances  $\ell \sim \mathcal{O}(10^3)$  m, the attainable laboratory values of  $|\mathbf{B}|$  are not strong enough to manifest the desirable effects. Gradually, the technology of high-intensity lasers is proving to be an alternative tool as it can achieve much stronger field strengths  $|\mathbf{B}| \sim \mathcal{O}(10^9)$  G in a short space-extension of the orders of  $\ell \sim \mathcal{O}(1-10)$   $\mu\text{m}$  allowing for the product  $|\mathbf{B}|\ell \sim \mathcal{O}(10^5 - 10^6)$  Gcm. However, this tiny interaction region could be compensated for by the envisaged ultrahigh intensities at future laser facilities. Contemporary projects such as the Extreme Light Infrastructure (ELI) [48] and the Exawatt Center for Extreme Light Studies (XCELS) [49] are being designed to reach the unprecedented level of  $|\mathbf{B}| \sim \mathcal{O}(10^{12})$  G, an order of magnitude below the critical magnetic field of QED  $B_c = 4.42 \times 10^{13}$  G, above which the superposition principle is no longer valid and the product  $|\mathbf{B}|\ell \sim \mathcal{O}(10^8 - 10^9)$  Gcm exceeds by an order of magnitude the maximum value resulting from experiments driven by a constant magnetic field. This has raised hopes that nonlinear effects including vacuum birefringence [50, 51], photon splitting [52], diffraction effects [53, 54, 55, 56, 57, 58] and the spontaneous production of electron-positron pairs from the vacuum [59, 60, 61] may soon be within an experimental scope with purely laser-based setups. There has been some important progress within the field of ALPs: some estimations have been put forward in [62, 63] and, recently, a more in-depth investigation has established stringent constraints on the coupling constant in regions of axion masses for which a laboratory setup based on dipole magnets provides less severe limits [64, 65].

Due to these considerations and motivated by the theoretical relevance of the ALPs, it is of interest to improve our understanding of photon-ALP(s) and ALP(s)-photon conversion in an experimentally attainable setup in which a high-intensity laser wave is taken as the background external field of the theory. This work contributes to this endeavor by focusing on the phenomenological aspects associated with pseudoscalar ALPs in the field of a circularly polarized monochromatic plane wave. Our main purpose is to explore the effects of these pseudoscalar particles on physical observables which can be used to improve the exclusion limits on its mass and coupling constant. To this end, we have organized the paper in the following form: in Sec. 2 the equations of motion associated with the oscillations processes are derived in the field of a plane wave of arbitrary shape. In addition, the low energy behavior of the vacuum polarization tensor is obtained from the Euler-Heisenberg Lagrangian in the one-loop and weak field approximations. This is followed by a particularization of the problem to the case in which the strong laser field is circularly polarized monochromatic plane wave. In Sec. 3, the corresponding dispersion relations and the equations of motion of fields involved in the Lagrangian are solved. This setup reveals that—contrary to what occurs in a pure QED context—chiral birefringence and dichroism of the vacuum are induced by the ALP-photon coupling. In Sec. 4 the observables associated with polarimetry techniques are derived and exclusion limits are then established. Finally, we present a summary and outlook of our research work.

## 2. Photon-Axion mixing in the field of a plane wave of arbitrary shape

Nonlinear effects of the electromagnetic field emerge as a consequence of effective couplings provided by the polarization of virtual electron-positron pairs. For small energy-momentum transfer, below the energy scale specified by the electron mass  $m_0$ , the physical phenomena associated with this theory can be described in a unitary way by means of the Euler-Heisenberg Lagrangian [66, 67]. For field strengths much weaker than the corresponding critical electric and magnetic fields, the leading behavior of this Lagrangian turns out to be<sup>1</sup>

$$\mathcal{L} = -\frac{1}{4\pi}\mathfrak{F} + \frac{1}{8\pi}\mathcal{L}_{\mathfrak{F}\mathfrak{F}}\mathfrak{F}^2 + \frac{1}{8\pi}\mathcal{L}_{\mathfrak{G}\mathfrak{G}}\mathfrak{G}^2, \quad (1)$$

<sup>1</sup>From now on natural and Gaussian units  $4\pi\epsilon_0 = \hbar = c = 1$  will be used.

where the quadratic terms in the field invariants  $\mathfrak{F} = \frac{1}{4}F_{\mu\nu}F^{\mu\nu}$  and  $\mathfrak{G} = \frac{1}{4}\tilde{F}_{\mu\nu}F^{\mu\nu}$  account for the quantum corrections to the Maxwell Lagrangian  $\mathcal{L}_M = -\frac{1}{4\pi}\mathfrak{F}$ , with  $F_{\mu\nu}$  the electromagnetic field tensor and  $\tilde{F}_{\mu\nu} = \frac{1}{2}\varepsilon_{\mu\nu\sigma\beta}F^{\sigma\beta}$  its dual. In the one-loop approximation, their respective coefficients are given by

$$\mathcal{L}_{\mathfrak{F}\mathfrak{F}} = \frac{4}{45}\frac{\alpha}{\pi}\frac{e^2}{m_0^4} \quad \text{and} \quad \mathcal{L}_{\mathfrak{G}\mathfrak{G}} = \frac{7}{45}\frac{\alpha}{\pi}\frac{e^2}{m_0^4}, \quad (2)$$

with  $\alpha = e^2 \approx 1/137$  the fine structure constant and  $e$  the absolute value of the electron charge.

The incorporation of an interacting pseudoscalar sector is usually done by preserving the fundamental symmetries of QED. In line with this assumption, the nonlinear effective action which describes the minimal coupling between the photon field  $A_\mu(x)$  and an ALP  $\phi$  reads

$$\mathcal{S} = \int d^4x \left\{ \mathcal{L} + \frac{1}{2}(\partial_\mu\phi)^2 - \frac{1}{2}m^2\phi^2 + \frac{g}{4\pi}\phi\mathfrak{G} \right\}, \quad (3)$$

where  $m$  and  $g \sim 1/\Lambda$  are the mass and coupling constant of the ALP, respectively. Here  $\Lambda$  is a parameter with dimension of energy, which for a QCD axion represents the phenomenological energy scale at which the Peccei-Quinn symmetry is broken [1].

### 2.1. Low energy behavior of the vacuum polarization tensor

Since we are interested in analyzing how this coupling modifies the propagation of small-amplitude electromagnetic waves  $a_\mu(x)$  in an external background field  $\mathcal{A}_\mu(x)$ , it is convenient to express  $A_\mu(x) = \mathcal{A}_\mu(x) + a_\mu(x)$  and expand  $\mathcal{S}$  in power series of  $a_\mu(x)$  above  $\mathcal{A}_\mu(x)$ . This procedure leads to the functional action

$$\mathcal{S}[a, \phi] = \int d^4x \left\{ \mathcal{L} - \frac{1}{2}\phi(\square + m^2)\phi + \frac{g}{8\pi}\phi\tilde{\mathcal{F}}_{\mu\nu}f^{\mu\nu} \right\}, \quad (4)$$

where  $f^{\mu\nu} = \partial^\mu a^\nu - \partial^\nu a^\mu$  and  $\mathcal{F}^{\mu\nu} = \partial^\mu \mathcal{A}^\nu - \partial^\nu \mathcal{A}^\mu$  are the electromagnetic tensors for small-amplitude waves and strong laser field, respectively. Here  $\square \equiv \partial^2/\partial t^2 - \nabla^2$ , and

$$\mathcal{L} = \frac{1}{2} \int d^4x' a^\mu(x) \mathcal{D}_{\mu\nu}^{-1}(x, x') a^\nu(x') \quad (5)$$

is the quadratic part of the effective Lagrangian in  $a_\mu(x)$ , with  $\mathcal{D}_{\mu\nu}^{-1}(x, x')$  denoting the inverse photon propagator in an external background field. Its general structure can be seen from the QED Schwinger-Dyson equations [68, 69, 70, 71, 72] and turns out to be

$$\mathcal{D}_{\mu\nu}^{-1}(x, x') = \frac{1}{4\pi} \left[ \square g_{\mu\nu} - \partial_\mu \partial_\nu \right] \delta^{(4)}(x - x') + \frac{1}{4\pi} \Pi_{\mu\nu}(x, x'). \quad (6)$$

Here  $g_{\mu\nu}$  is the metric tensor whose diagonal components are  $g^{11} = g^{22} = g^{33} = -g^{00} = -1$ . Obviously, the first term in Eq. (6) gives the Maxwell Lagrangian while the second is responsible for the quantum corrections which, for small-amplitude electromagnetic waves, are described by the vacuum polarization tensor  $\Pi_{\mu\nu}(x, x')$ .

To reveal the low energy behavior of this tensor and obtain a clear picture of the photon spectrum it is sufficient to variate the action [Eq. (3)] with respect to  $A_\nu(x)$  twice, set the field invariants  $\mathfrak{F}$ ,  $\mathfrak{G}$  and  $\phi$  to zero, and compare the resulting expression to Eq. (6). The former evaluation is in correspondence with the fact that for plane waves–crossed field, equal strengths–the field invariants  $\mathfrak{F}$  and  $\mathfrak{G}$  vanish identically. In contrast, by setting  $\phi = 0$  we are assuming that there is no expectation for the axion fields permeating the universe, or that such vacuum expectation value is neglectable in comparison with the fluctuations in which we are interested<sup>2</sup>. As long as this is the case, we find that

$$\Pi_{\mu\nu}(x, x') = - \left\{ \mathcal{L}_{\mathfrak{F}\mathfrak{F}} \mathcal{F}_{\beta\nu} \mathcal{F}_{\alpha\mu} \partial^\alpha \partial^\beta + \mathcal{L}_{\mathfrak{G}\mathfrak{G}} \tilde{\mathcal{F}}_{\beta\nu} \tilde{\mathcal{F}}_{\alpha\mu} \partial^\alpha \partial^\beta \right\} \delta^{(4)}(x - x'), \quad (7)$$

<sup>2</sup>A nonvanishing expectation value of  $\phi$  might play a relevant role when axions are considered as dark matter candidates [9].

where the following relation  $\mathcal{F}^{\mu\nu}\partial_\mu\mathcal{F}_{\lambda\rho}\propto\kappa_\mu\mathcal{F}^{\mu\nu}=0$  has been used. The procedure used to obtain the expression above has also been successfully applied to the case of constant background fields [73, 74]. This is applicable as long as the electromagnetic field is slowly varying on a linear spacetime scale of the order of the Compton-wavelength  $\lambda_c=1/m_0=3.9\times 10^{-11}\text{cm}$ , otherwise the spatial and temporal dispersion become important issues and one is forced to consider the general expression of  $\Pi_{\mu\nu}$  calculated from Feynman diagram techniques [see Fig. (1)] in the Furry picture. This calculation was originally carried out by Batalin and Shabad [75] in the special case of a constant electromagnetic field. In contrast, Baier, Mil'shtein and Strakhovenko [76] (see also [77, 78]) were the first to determine  $\Pi_{\mu\nu}$  in the field of a plane-wave of the form

$$\mathcal{A}^\mu(x)=a_1^\mu\psi_1(\kappa x)+a_2^\mu\psi_2(\kappa x). \quad (8)$$

Here  $a_{1,2}$  are the amplitudes of the strong laser wave,  $\kappa^\mu=(\kappa^0,\boldsymbol{\kappa})$  denotes its four-momentum while  $\psi_{1,2}$  are arbitrary functions which characterize the shape of the laser field. The latter quantities additionally fulfill the following constraints:

$$\kappa^2=0, \quad \kappa a_1=\kappa a_2=a_1 a_2=0. \quad (9)$$

In this context, the external field tensor of the wave [Eq. (8)] is  $\mathcal{F}^{\mu\nu}=\sum_{i=1,2}\mathcal{F}_i^{\mu\nu}\psi'_i(\varphi)$ ,  $\mathcal{F}_i^{\mu\nu}=\kappa^\mu a_i^\nu-\kappa^\nu a_i^\mu$ , with  $\varphi\equiv\kappa x$  and  $\psi'_i(\varphi)\equiv d\psi_i/d\varphi$ . It is worth noting at this point that the constant electric [ $E_i^j=\mathcal{F}_i^{j0}$ ] and magnetic [ $\mathcal{F}_i^{jk}=-\epsilon^{jkl}B_l^k$ ] amplitudes associated with each term in Eq. (8) are crossed, orthogonal and with the same strength  $|\mathbf{E}_i|=|\mathbf{B}_i|$ .

In the present paper the field described above is also considered as the external background of the theory. Due to this fact the tensorial structure of  $\Pi_{\mu\nu}$  can be written in terms of Lorentz covariant vectors  $\Lambda_i^\mu$  ( $i=1,2,3,4$ ):

$$\Pi^{\mu\nu}(k_1,k_2)=c_1\Lambda_1^\mu\Lambda_2^\nu+c_2\Lambda_2^\mu\Lambda_1^\nu+c_3\Lambda_1^\mu\Lambda_1^\nu+c_4\Lambda_2^\mu\Lambda_2^\nu+c_5\Lambda_3^\mu\Lambda_4^\nu \quad (10)$$

It is worth mentioning at this point that  $\Lambda_i^\mu$  were constructed to satisfy the first principles of charge conjugation, spatial and time reversal symmetry as well as gauge and Poincaré invariances in the polarization tensor. Following the notation used in [76] we write

$$\Lambda_1^\mu(k)=-\frac{\mathcal{F}_1^{\mu\nu}k_\nu}{(k\kappa)(-a_1^2)^{1/2}}, \quad \Lambda_2^\mu(k)=-\frac{\mathcal{F}_2^{\mu\nu}k_\nu}{(k\kappa)(-a_2^2)^{1/2}}, \quad \Lambda_3^\mu(k)=\frac{\kappa^\mu k_1^2-k_1^\mu(k\kappa)}{(k\kappa)(k_1^2)^{1/2}}, \quad \Lambda_4^\mu(k)=\frac{\kappa^\mu k_2^2-k_2^\mu(k\kappa)}{(k\kappa)(k_2^2)^{1/2}}. \quad (11)$$

Note that the short-hand notation  $k$  in the expressions above may stand for either  $k_1$  or  $k_2$ . It is important to note that the vectors  $\Lambda_1(k_1)$ ,  $\Lambda_2(k_1)$  and  $\Lambda_3(k_1)$  are orthogonal to each other,  $\Lambda_i^\mu(k_1)\Lambda_{j\mu}(k_1)=-\delta_{ij}$ , and fulfill the completeness relation

$$g^{\mu\nu}-\frac{k_1^\mu k_1^\nu}{k_1^2}=-\sum_{i=1}^3\Lambda_i^\mu(k_1)\Lambda_i^\nu(k_1). \quad (12)$$

A similar statement applies if the set of vectors  $\Lambda_1(k_2)$ ,  $\Lambda_2(k_2)$  and  $\Lambda_4(k_2)$  are considered.

Now, in Eq. (10) the form factor  $c_i$  is a distribution function which depends on the fundamental scalars of the theory:  $k^2$ ,  $\kappa k$  and  $\xi_j^2=-e^2 a_j^2/m_0^2$ . In order to determine its low energy behavior it is convenient to express the

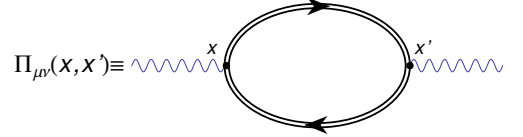


Figure 1: Diagrammatic representation of the vacuum polarization tensor. The double lines represent the electron-positron Green's functions including the interaction with the external field. The two wavy lines denote the amputated legs corresponding to the small-amplitude electromagnetic waves.

Fourier transformation of Eq. (7) as

$$\begin{aligned}
\Pi^{\mu\nu}(k_1, k_2) = & - \mathcal{L}_{\mathfrak{F}\mathfrak{F}}(\varkappa k_1)^2 \left\{ a_1^2 \Lambda_1^\mu \Lambda_1^\nu \int d^4 p \psi'_1(p) \psi'_1(k_1 - k_2 - p) - (-a_1^2)^{1/2} (-a_2^2)^{1/2} (\Lambda_1^\mu \Lambda_2^\nu + \Lambda_2^\mu \Lambda_1^\nu) \right. \\
& \times \int d^4 p \psi'_1(p) \psi'_2(k_1 - k_2 - p) + a_2^2 \Lambda_2^\mu \Lambda_2^\nu \int d^4 p \psi'_2(p) \psi'_2(k_1 - k_2 - p) \left. \right\} - \mathcal{L}_{\mathfrak{G}\mathfrak{G}}(\varkappa k_1)^2 \left\{ a_1^2 \tilde{\Lambda}_1^\mu \tilde{\Lambda}_1^\mu \right. \\
& \times \int d^4 p \psi'_1(p) \psi'_1(k_1 - k_2 - p) - (-a_1^2)^{1/2} (-a_2^2)^{1/2} (\tilde{\Lambda}_1^\mu \tilde{\Lambda}_2^\nu + \tilde{\Lambda}_2^\mu \tilde{\Lambda}_1^\nu) \int d^4 p \psi'_1(p) \psi'_2(k_1 - k_2 - p) \\
& \left. + a_2^2 \tilde{\Lambda}_2^\mu \tilde{\Lambda}_2^\nu \int d^4 p \psi'_2(p) \psi'_2(k_1 - k_2 - p) \right\}, \tag{13}
\end{aligned}$$

where  $\psi'_i(q)$  must be understood as the Fourier transform of  $\psi'_i(\varphi) = d\psi_i(\varphi)/d\varphi$ . Note that the shorthand notation  $d^4 p \equiv d^4 p/(2\pi)^4$  as well as the two pseudovectors

$$\tilde{\Lambda}_1^\mu(k) = -\frac{\tilde{\mathcal{F}}_1^{\mu\nu} k_\nu}{(k\varkappa)(-a_1^2)^{1/2}}, \quad \tilde{\Lambda}_2^\mu(k) = -\frac{\tilde{\mathcal{F}}_2^{\mu\nu} k_\nu}{(k\varkappa)(-a_2^2)^{1/2}} \tag{14}$$

have been introduced. They are orthonormalized according to  $\tilde{\Lambda}_i \tilde{\Lambda}_j = -\delta_{ij}$  and satisfy the relations

$$\tilde{\Lambda}_i \Lambda_j = -\epsilon_{ij}, \quad \tilde{\Lambda}_i \Lambda_3 = 0 \quad \text{for } i, j = 1, 2, \tag{15}$$

with the antisymmetric tensor  $\epsilon_{ij}$  taken as  $\epsilon_{12} = -\epsilon_{21} = 1$ . We then project  $\Pi_{\mu\nu}(k_1, k_2)$  with the appropriate combinations of the vectors  $\Lambda_1 \dots \Lambda_4$  appearing in Eq. (10). Guided by this procedure we find that

$$c_1 = c_2, \quad c_3 = c_4(1 \leftrightarrow 2), \quad c_5 = 0, \quad c_2 = -\frac{1}{15} \frac{\alpha}{\pi} \frac{(k\varkappa)^2}{m_0^2} \xi_1 \xi_2 \int d^4 q \psi'_1(q) \psi'_2(k_1 - k_2 - q), \tag{16}$$

$$c_4 = \frac{4}{45} \frac{\alpha}{\pi} \frac{(k\varkappa)^2}{m_0^2} \xi_2^2 \int d^4 q \psi'_2(q) \psi'_2(k_1 - k_2 - q) + \frac{7}{45} \frac{\alpha}{\pi} \frac{(k\varkappa)^2}{m_0^2} \xi_1^2 \int d^4 q \psi'_1(q) \psi'_1(k_1 - k_2 - q). \tag{17}$$

We want to stress that the derivation of these coefficients requires the use of the orthogonal character of the four-vectors  $\Lambda_i$ , as well as Eq. (15).

The previous results show that the final structure of the vacuum polarization tensor in the field of a plane-wave [Eq. (8)] depends on its specific shape. This statement is manifest through the absence of the usual Dirac delta functions which impose energy and momentum conservation. Therefore the interaction with a strong laser field could, in general, involve inelastic scattering.

## 2.2. Equations of motion and general considerations in the case of an circularly polarized monochromatic wave

Let us turn our attention to the equations of motion associated with our problem. These can be derived from the Lagrangian [Eq. (4)] and turn out to be coupled to each other. Indeed, in Landau gauge  $\partial_\mu a^\mu = 0$  they read

$$(\square + m^2) \phi - \frac{g}{8\pi} \tilde{\mathcal{F}}_{\mu\nu} f^{\mu\nu} = 0, \tag{18}$$

$$\square a_\mu(x) + \int d^4 x' \Pi_{\mu\nu}(x, x') a^\nu(x') + g \tilde{\mathcal{F}}_{\mu\nu} \partial^\nu \phi = 0. \tag{19}$$

The first equation shows that a small-amplitude electromagnetic wave can be converted into an axion via the corresponding coupling through the dual of the external field tensor. The second equation, however, allows a reconversion process in which the axion becomes a propagating photon again. In order to analyze such processes it is convenient to transform into momentum space. In this context, Eqs. (18) and (19) are converted into algebraic forms

$$0 = \Delta^{-1}(k) \phi(k) + \frac{ig}{4\pi} \sum_{i=1,2} \tilde{\Lambda}_i^\mu \varrho_i^{1/2} \int d^4 p \psi'_i(p) a_\mu(k-p), \tag{20}$$

$$0 = k^2 a^\mu(k) - \int d^4 q \Pi^{\mu\nu}(k, q) a_\nu(q) + ig \sum_{i=1,2} \tilde{\Lambda}_i^\mu \varrho_i^{1/2} \int d^4 p \psi'_i(p) \phi(k-p) \tag{21}$$

where  $\varrho_i \equiv k_1 \mathcal{F}_i^2 k_1 = k_1 \tilde{\mathcal{F}}_i^2 k_1$  is a Lorentz scalar whose explicit structure reads

$$\varrho_i = -(k\kappa)^2 a_i^2 \quad (22)$$

and  $\Delta^{-1}(k) = k^2 - m^2$  is the inverse axion propagator. Note that the axion-photon coupling is provided by the pseudovectors  $\tilde{\Lambda}_{1,2}$  which preserve parity invariance. Conversely, if the minimal coupling in Eq. (3) is replaced by a parity preserving interaction involving a scalar ALP, i.e.,  $\sim g\phi\mathcal{F}$ , the mixing term in Eq. (4) acquires a structure  $\sim \frac{g}{8\pi} \mathcal{F}^{\mu\nu} f_{\mu\nu}$ . Following a procedure similar to that used in this section we obtain a system of equations similar to those given in Eqs. (20-21), the only difference arising in the last term, which now involves  $\Lambda_i$  instead of  $\tilde{\Lambda}_i$ .

Let us consider the case in which the parameters  $\xi_{1,2}$  and the functions  $\psi_{1,2}$  are chosen so that the external laser field is an circularly polarized monochromatic wave. In our framework this corresponds to take  $\xi^2 \equiv \xi_1^2 = \xi_2^2$ ,  $\psi_1 = \cos(\varphi)$  and  $\psi_2 = \sin(\varphi)$  with

$$\psi'_1(p) = \frac{1}{2i} [\delta^{(4)}(p + \kappa) - \delta^{(4)}(p - \kappa)], \quad \psi'_2(p) = \frac{1}{2} [\delta^{(4)}(p + \kappa) + \delta^{(4)}(p - \kappa)], \quad (23)$$

and  $\delta^{(4)}(x) \equiv (2\pi)^4 \delta^{(4)}(x)$ . This particular context allows for introducing the following covariant vectors:

$$\Lambda_{\pm}^{\mu} = \Lambda_1^{\mu} \pm i\Lambda_2^{\mu} \quad \text{and} \quad \tilde{\Lambda}_{\pm}^{\mu} = \tilde{\Lambda}_1^{\mu} \pm i\tilde{\Lambda}_2^{\mu}, \quad (24)$$

where  $\Lambda_{1,2}$  are given in Eq. (11). Note that the new vectors in Eq. (24) satisfy the relations

$$\Lambda_+ \Lambda_- = -2, \quad \tilde{\Lambda}_+ \Lambda_- = -\tilde{\Lambda}_- \Lambda_+ = 2i, \quad \Lambda_+ \Lambda_+ = \Lambda_- \Lambda_- = \Lambda_+ \tilde{\Lambda}_+ = \Lambda_- \tilde{\Lambda}_- = 0. \quad (25)$$

At this point, it is worth noting that the low energy behavior of the vacuum polarization tensor can be written as

$$\begin{aligned} \Pi^{\mu\nu}(k_1, k_2) &= \sum_{n=0,+,-} \Pi_n^{\mu\nu} \delta^{(4)}(k_1 - k_2 + 2n\kappa), \\ \Pi_0^{\mu\nu} &= \pi_3 (\Lambda_1^{\mu} \Lambda_1^{\nu} + \Lambda_2^{\mu} \Lambda_2^{\nu}), \quad \Pi_{\pm}^{\mu\nu} = \pi_0 \Lambda_{\pm}^{\mu} \Lambda_{\pm}^{\nu}, \quad \pi_3 = \frac{11}{90} \frac{\alpha}{\pi} \frac{(\kappa k)^2}{m_0^2} \xi^2, \quad \pi_0 = \frac{1}{60} \frac{\alpha}{\pi} \frac{(\kappa k)^2}{m_0^2} \xi^2. \end{aligned} \quad (26)$$

The structure of these entities coincides with those obtained by Bařer, Mil'shteĭn and Strakhovenko in [76] - according to the correspondence  $\pi_3 \leftrightarrow \alpha_3$  and  $\pi_0 \leftrightarrow \alpha_0$ . Observe that the tensorial structures  $\Pi_n^{\mu\nu}$  are in correspondence with the possible states of helicity  $n = 0, +, -$ .

Eq. (26) warrants further comment. Firstly, it may be seen that the scattered field is emitted with three different frequencies. One of these coincides with the frequency of the incoming small-amplitude wave, resulting in an elastic scattering. The remaining two frequencies emerge as a consequence of inelastic processes in which the emission and absorption of two laser photons occur. These turn out to be shifted to lower and higher values in comparison with the original monochromatic frequency. The scattering of light in these latter two cases is analogous to the Raman process in molecular physics with  $\kappa_0$  imitating the vibrational frequency of the molecules. Similarly, it might be used to test the nonlinear properties of the QED vacuum. In fact, the associated spectroscopy has been recently put forward as alternative way of probing the predicted vacuum of minicharged particles [79].

In order to pursue our research we insert Eqs. (23) and (26) into Eqs. (20) and (21), arriving at the following equation for the photon-axion

$$\Delta^{-1}(k)\phi(k) - \frac{g}{8\pi} \varrho^{1/2} \tilde{\Lambda}_-^{\mu} a_{\mu}(k - \kappa) + \frac{g}{8\pi} \varrho^{1/2} \tilde{\Lambda}_+^{\mu} a_{\mu}(k + \kappa) = 0, \quad (27)$$

and axion-photon conversion

$$k^2 a^{\mu}(k) + \frac{1}{2} g \varrho^{1/2} [\tilde{\Lambda}_+^{\mu} \phi(k + \kappa) - \tilde{\Lambda}_-^{\mu} \phi(k - \kappa)] - \sum_{\lambda=0,+,-} \Pi_{\lambda}^{\mu\nu}(k) a_{\nu}(k + 2\lambda\kappa) = 0, \quad (28)$$

where  $\varrho \equiv \varrho_1 = \varrho_2$  is the Lorentz scalar given in Eq. (22). These last two equations constitute our starting point for the following analyses. They reveal that the conversion process changes the momentum content. Thus, in presence of

a circularly polarized monochromatic wave the mixing phenomenon is conceptually more involved than in the case of a constant magnetic field.

The solution of our problem can be written as a superposition of two transverse waves

$$a^\mu(k) = \frac{f_+(k)}{\sqrt{2}} \Lambda_+^\mu + \frac{f_-(k)}{\sqrt{2}} \Lambda_-^\mu. \quad (29)$$

Two additional terms may be included in this expansion. However, both are associated with longitudinal and nonphysical propagation modes. One of these terms is longitudinal by construction  $\sim k^\mu$ ; while the remaining is transverse and proportional to  $\Lambda_3^\mu$ , the absence of  $c_5$  in Eq. (26) [compare with Eq. (10)] leads to a trivial dispersion equation  $k^2 = 0$  and so  $\Lambda_3^\mu \sim k^\mu$  [see Eq. (11)] becomes a longitudinal gauge mode. As such, both solutions have been omitted.

We substitute Eq. (29) into Eqs. (27)-(28) and multiply  $\Lambda_\pm^\mu$  by the left-hand side of Eq. (28). As a consequence, the resulting system of equations to be analyzed is

$$\mathcal{G}^{(i)}(k) \mathbf{z}^{(i)}(k) = 0 \quad \text{with} \quad i = 1, 2. \quad (30)$$

Here the quantities involved are defined as follows

$$\mathcal{G}^{(1)}(k) = \begin{bmatrix} \Delta^{-1}(k + \varkappa) & \frac{i\sqrt{2}}{8\pi} g\mathcal{Q}^{1/2} & \frac{i\sqrt{2}}{8\pi} g\mathcal{Q}^{1/2} \\ -\frac{i\sqrt{2}}{2} g\mathcal{Q}^{1/2} & k^2 + \pi_3 & 2\pi_0 \\ -\frac{i\sqrt{2}}{2} g\mathcal{Q}^{1/2} & 2\pi_0 & (k + 2\varkappa)^2 + \pi_3 \end{bmatrix}, \quad \mathcal{G}^{(2)}(k) = \begin{bmatrix} \Delta^{-1}(k - \varkappa) & \frac{i\sqrt{2}}{8\pi} g\mathcal{Q}^{1/2} & \frac{i\sqrt{2}}{8\pi} g\mathcal{Q}^{1/2} \\ -\frac{i\sqrt{2}}{2} g\mathcal{Q}^{1/2} & (k - 2\varkappa)^2 + \pi_3 & 2\pi_0 \\ -\frac{i\sqrt{2}}{2} g\mathcal{Q}^{1/2} & 2\pi_0 & k^2 + \pi_3 \end{bmatrix}, \quad (31)$$

$$\mathbf{z}^{(1)} = \begin{bmatrix} \phi(k + \varkappa) \\ f_+(k) \\ f_-(k + 2\varkappa) \end{bmatrix}, \quad \mathbf{z}^{(2)} = \begin{bmatrix} \phi(k - \varkappa) \\ f_+(k - 2\varkappa) \\ f_-(k) \end{bmatrix}. \quad (32)$$

It is remarkable that both eigenproblems are correlated by means of the relations

$$\mathcal{G}^{(1)}(k - 2\varkappa) \mathbf{z}^{(1)}(k - 2\varkappa) = \mathcal{G}^{(2)}(k) \mathbf{z}^{(2)}(k) = 0 \quad \text{and} \quad \mathcal{G}^{(2)}(k + 2\varkappa) \mathbf{z}^{(2)}(k + 2\varkappa) = \mathcal{G}^{(1)}(k) \mathbf{z}^{(1)}(k) = 0.$$

We point out that the field components contained in these vectors cannot be understood as mass eigenmodes. Once the ALP-photon coupling is considered they become—as occurs in the neutrino oscillations [80]—“flavor” eigenstates. This means that the fields in the Lagrangian are not equivalent to the mass eigenstates/propagating modes of the interacting theory.

### 3. Oscillations

#### 3.1. Isolating the ALP-induced vacuum birefringence

Nontrivial solutions of the mixing process emerge whenever the determinant of  $\mathcal{G}^{(1)}(k)$  vanishes identically. In such a case, a cubic equation in  $k^2$  (sextic in the frequency  $\omega$ ) is generated:

$$(k^2 + \pi_3) [k^2 - m^2 + 2(k\varkappa)] [(k + 2\varkappa)^2 + \pi_3] = \frac{g^2}{4\pi} \mathcal{Q} [k^2 + 2(k\varkappa)], \quad (33)$$

where the dispersion equation for the strong wave, i.e.,  $\varkappa^2 = 0$  has been used. Moreover, this outcome has been derived by neglecting those terms resulting from the off-diagonal components of  $\mathcal{G}^{(1)}(k)$  which are proportional to  $\sim \alpha^2$  and  $\sim g^2\alpha$ . Note that the left-hand side of this equation still contain contributions that will be eventually disregarded as, e.g., a term proportional to  $\sim \pi_3^2$ . Certainly, the exact solutions of Eq. (33) can be determined by analytical procedures. However, we are interested in analyzing the physical context in which the ALP-photon coupling does not dramatically modify the free dispersion relations of the particles involved. Accordingly, one can manipulate the right-hand side in Eq. (33) as a small perturbative correction to the leading equations which result when the ALP-photon coupling vanishes identically. This assumption allows us to apply a recursive method where the following set of equations

$$k^2 = 0, \quad (34)$$

$$k^2 - m^2 + 2(k\varkappa) = 0 \quad (35)$$

is taken as the starting point. In this framework, two massless modes are found<sup>3</sup>. The first is determined by passing the square brackets in Eq. (33) to the right-hand side. We use Eq. (34) to express the resulting equation as follows

$$k^2 \simeq -\pi_3 + \frac{g^2 \varrho}{8\pi(2k\mathcal{I} - m^2)}. \quad (36)$$

The left-hand side of this expression is then linearized with respect to  $\omega$  by approaching  $k^2 = \omega^2 - \mathbf{k}^2 = (\omega - |\mathbf{k}|)(\omega + |\mathbf{k}|) \approx 2|\mathbf{k}|(\omega - |\mathbf{k}|)$ . We additionally set, the momentum  $k$  involved on the right-hand side of this equation to  $k = \mathcal{I} \equiv (\omega_{\mathbf{k}}, \mathbf{k})$  with  $\omega_{\mathbf{k}} \equiv |\mathbf{k}|$ . As a consequence the dispersion relation is found to be

$$\omega_+^{(1)}(\mathbf{k}) \approx \omega_{\mathbf{k}} - \frac{\pi_3}{2\omega_{\mathbf{k}}} + \frac{g^2(\mathcal{I}\mathcal{I})^2 I}{4\mathcal{I}_0^2 \omega_{\mathbf{k}} [2(\mathcal{I}\mathcal{I}) - m^2]}, \quad (37)$$

where  $I = E^2/4\pi = \mathcal{I}_0^2 \mathbf{a}^2/(4\pi)$  denotes the peak intensity associated with strong field of the wave<sup>4</sup>. The second massless solution can be determined by moving the first two brackets in Eq. (33) to its right-hand side and setting  $k = \mathcal{I} + 2\mathcal{I}$ . We then use the linearization

$$(k + 2\mathcal{I})^2 \simeq 2\omega_{\mathbf{k}+2\mathcal{I}} (\omega - \omega_{\mathbf{k}+2\mathcal{I}} + 2\mathcal{I}_0), \quad (38)$$

which applies for  $k\mathcal{I} \simeq 0$ . As a consequence, it follows

$$\omega_-^{(1)}(\mathbf{k} + 2\mathcal{I}) = \omega_{\mathbf{k}+2\mathcal{I}} - 2\mathcal{I}_0 - \frac{\pi_3}{2\omega_{\mathbf{k}+2\mathcal{I}}} - \frac{g^2(\mathcal{I}\mathcal{I})^2 I}{4\mathcal{I}_0^2 \omega_{\mathbf{k}+2\mathcal{I}} [2(\mathcal{I}\mathcal{I}) + m^2]}, \quad (39)$$

where the short-hand notation  $\omega_{\mathbf{k}+2\mathcal{I}} \equiv |\mathbf{k} + 2\mathcal{I}|$  has been introduced. Note that the subindices of  $\omega_{\pm}^{(1)}$  have been added to establish a correspondence between the dispersion relations and the helicity states.

Some comments are in order. Firstly in the limit where  $\omega_{\mathbf{k}} \rightarrow 0$  the dispersion relations [Eqs. (37) and (39)] become trivial. As such gauge invariance is preserved and one can identify Eqs. (37) and (39) as the photon-like solutions of the mixing process. The pole in the interacting term of  $\omega_+^{(1)}(\mathbf{k})$  also deserves some attention. This translates into an ALP mass depending not only upon the momentum of the probe laser beam but also on the frequency of the strong background field

$$m_* = (2\mathcal{I}\mathcal{I})^{1/2}. \quad (40)$$

When the above condition is fulfilled the dispersion relation Eq. (37) is resonantly enhanced. Obviously, this is not consistent with our perturbative treatment. However, Eq. (37) can be used to explore the domains in which the ALP mass is near resonance, i.e.,  $m = m_* \pm \epsilon$ ,  $\epsilon > 0$  provided the condition

$$m_* \gg \epsilon \gg \frac{g^2 m_*^3 I}{32\mathcal{I}_0^2 \omega_{\mathbf{k}}^2}. \quad (41)$$

Otherwise the use of our perturbative approach would not be justified. Nevertheless, whenever the collision angle between the two waves is tiny [ $\theta \ll 1$ ], small resonant masses might be explored:

$$m_* \simeq \theta(\omega_{\mathbf{k}}\mathcal{I}_0)^{1/2}. \quad (42)$$

However, less stringent constraints in the coupling constant  $g$  are expected to appear because the interaction becomes extremely small  $\sim \theta^3$ . This case will be treated shortly.

Our original dispersion equation [Eq. (33)] also allows for massive solutions. In order to determine which of them are physical, we first note that Eq. (35) provides two frequencies. We discard the one which is negative when the external field frequency tends to zero. In correspondence, we obtain

$$\omega_+ = \varepsilon_{\mathbf{k}+\mathcal{I}} - \mathcal{I}_0, \quad \varepsilon_{\mathbf{k}+\mathcal{I}} = \left[ (\omega_{\mathbf{k}} + \mathcal{I}_0)^2 + m^2 - m_*^2 \right]^{1/2}. \quad (43)$$

<sup>3</sup>This result is somewhat expected, starting with two photon modes, a massive axion mode and assuming a tiny coupling/mixing.

<sup>4</sup>Observe that the temporal gauge, i.e.,  $a_0 = 0$  has been chosen.



This expression is in agreement with the energy-momentum conservation whose balance at tree level reads

$$k + \varkappa = p_+ \quad \text{with} \quad p_+^\mu = (\varepsilon_{\mathbf{p}}, \mathbf{p}).$$

As long as Eq. (34) is taken into account, the above relation promotes the resonant condition  $m^2 = m_*^2$ . Observe that, in the vicinity of the resonance,  $m^2 - m_*^2 \approx 2m_*\varepsilon$  and in correspondence Eq. (43) can be written as

$$\omega_+ \approx \omega_{\mathbf{k}} + \frac{1}{2} \frac{m^2 - m_*^2}{\omega_{\mathbf{k}} + \varkappa_0}, \quad (44)$$

where the second term must be understood as a very small contribution with  $(\omega_{\mathbf{k}} + \varkappa_0)^2 \gg 2\varepsilon m_*$ . The correction to Eq. (44) due to the ALP-photon coupling can be found similarly to how the massless modes were determined. Using the linearization  $k^2 + m_*^2 - m^2 \approx 2\varepsilon_{\mathbf{k}+\varkappa}(\omega - \omega_+)$ , we find that the massive solution of Eq. (33)–up to first nontrivial order in  $g^2$ –is given by

$$w_0^{(1)}(\mathbf{k}) \approx \omega_{\mathbf{k}} + \frac{1}{2} \frac{m^2 - m_*^2}{\omega_{\mathbf{k}} + \varkappa_0} + \frac{g^2 I m^2 m_*^4}{8\varkappa_0^2 \varepsilon_{\mathbf{k}+\varkappa} [m^4 - m_*^4]}. \quad (45)$$

The above expression diverges when the mass coincides with the resonant one [Eq. (40)]. However, similar to the massless mode [Eq. (39)], it can be exploited to investigate the ALP-photon oscillations near resonance, provided Eq. (41) is satisfied.

In order to determine the solutions of the remaining eigenproblem, the determinant of  $\mathcal{G}^{(2)}$  must vanish. This condition generates the dispersion equation

$$(k^2 + \pi_3) [k^2 - m^2 - 2(k\varkappa)] [(k - 2\varkappa)^2 + \pi_3] = \frac{g^2}{4\pi} \rho [k^2 - 2(k\varkappa)]. \quad (46)$$

The recursive procedure described above allows us to find a photon-like solution associated with the negative helicity mode

$$w_-^{(2)}(\mathbf{k}) \approx \omega_{\mathbf{k}} - \frac{\pi_3}{2\omega_{\mathbf{k}}} - \frac{g^2 m_*^4 I}{16\varkappa_0^2 \omega_{\mathbf{k}} [m_*^2 + m^2]}. \quad (47)$$

In contrast, the dispersion law for a photon-like state with positive helicity and momentum  $\mathbf{k} - 2\varkappa$  reads

$$w_+^{(2)}(\mathbf{k} - 2\varkappa) \approx \omega_{\mathbf{k}-2\varkappa} + 2\varkappa_0 - \frac{\pi_3}{2\omega_{\mathbf{k}-2\varkappa}} + \frac{g^2 m_*^4 I}{16\varkappa_0^2 \omega_{\mathbf{k}-2\varkappa} [m_*^2 - m^2]}, \quad (48)$$

where  $\omega_{\mathbf{k}-2\varkappa} = |\mathbf{k} - 2\varkappa|$ . Clearly, another massive solution arises from Eq. (46). The starting point for finding out this dispersion law is the leading order equation  $k^2 - 2k\varkappa - m^2 = 0$ . Among its solutions, the following becomes noticeable

$$\omega_- = \varepsilon_{\mathbf{k}-\varkappa} + \varkappa_0, \quad \varepsilon_{\mathbf{k}-\varkappa} = [(\omega_{\mathbf{k}} - \varkappa_0)^2 + m_*^2 + m^2]^{1/2}. \quad (49)$$

This describes the energy conservation of a hypothetical mixing where the probe beam emits a photon of the strong wave. This kind of oscillations are kinematically forbidden at tree level since the energy-momentum balance  $k - \varkappa = p_-$  with  $p_-^\mu = (\varepsilon_{\mathbf{p}}, \mathbf{p})$  implies a process where the ALP mass is negative  $m^2 = -m_*^2 \leq 0$ . Once the corrections coming from the vacuum polarization and the ALP-photon interaction are incorporated, the dispersion equation [Eq. (46)] replaces the previous condition and another massive solution could arise. In Sec. 3.3 we will show that the nonoccurrence of the aforementioned process—at tree level—is intrinsically associated with the monochromaticity of the strong wave [Eq. (8)], a fact which formally restricts us to work in the limit of infinite pulse length. Nevertheless, in practice the interaction time is always finite, the strong wave is not monochromatic and, consequently, one can approach the remaining massive solution by

$$w_0^{(2)}(\mathbf{k}) \approx \omega_{\mathbf{k}} + \frac{1}{2} \frac{m^2 + m_*^2}{\omega_{\mathbf{k}} - \varkappa_0} + \frac{g^2 I m^2 m_*^4}{8\varkappa_0^2 \varepsilon_{\mathbf{k}-\varkappa} [m^4 - m_*^4]}, \quad (50)$$

where the approximation  $(\omega_{\mathbf{k}} - \varkappa_0)^2 \gg m^2 + m_*^2$  has been used. Clearly, in the limit of  $g \rightarrow 0$  the above dispersion relation reduces to a nonphysical tree level condition which is connected to Eq. (49). However, we will see very shortly that in such a context, a vanishing probability of conversion is obtained. Moreover, it will be shown that, as soon as the ALP-photon interaction is taken into account, the probability that a probe photon oscillates into  $\phi(k - \varkappa)$  is very small in comparison with the remaining possibility of mixing, i.e., when  $\phi(k + \varkappa)$  is involved. This situation is somewhat expected: among the massive-like solutions  $w_0^{(1)}(\mathbf{k})$  defines the state with minimal energy. Hence, the conversion of a photon into a massive mode with energy  $w_0^{(2)}$  is less likely to occur.

To conclude this subsection we determine the phase velocity  $v_{\pm} = w_{\pm}(\mathbf{k})/|\mathbf{k}|$  associated with each massless propagation mode, i.e., Eqs. (37) and (47). In this case we find

$$v_{\pm} = 1 - \frac{\pi_3}{2\omega_{\mathbf{k}}^2} \pm \frac{g^2 m_*^4 I}{16\varkappa_0^2 \omega_{\mathbf{k}}^2 (m_*^2 \mp m^2)}. \quad (51)$$

Obviously, in the absence of the ALP-photon coupling, both modes propagate with the same phase velocity  $v_{\pm} \simeq 1 - \pi_3/2\omega_{\mathbf{k}}^2$ . This implies that, at lower energy-momentum transfer [ $\omega_{\mathbf{k}}, \varkappa_0 \ll m_0$ ] and in the weak field approximation [ $E \ll E_c$ ], the QED vacuum in the field of a circular polarized wave—in leading order—behaves as an isotropic non-birefringent medium. This situation, however, is reverted when the ALP-photon coupling is considered. In fact, the last term in Eq. (51) manifests that the plausible emission and absorption of virtual ALPs with different momentum content induces a chiral-like birefringence.

### 3.2. The flavor-like states

The previous linearizations in the dispersion equations are equivalents to reduce the differential order in the equations of motion [Eqs. (18)-(19)]. In correspondence, we can approach the first flavor-like state in Eq. (32) as a superposition of the three mass eigenstates which characterize the mixing process

$$\mathbf{z}^{(1)}(\omega) \simeq \sum_{\lambda=0,+,-} \mathcal{N}_{\lambda}^{(1)} \mathbf{z}_{\lambda}^{(1)} \delta(\omega - w_{\lambda}^{(1)}). \quad (52)$$

While  $\mathcal{N}_{\lambda}^{(1)}$  denote some constants to be determined by the initial conditions,  $\mathbf{z}_{\lambda}^{(1)}$  represent the normalized eigenstates of  $\mathcal{G}^{(1)}$ :

$$\mathbf{z}_{+}^{(1)} = \frac{[i \tan(\theta_{+}^{(1)}), 1, -\tan(\varphi_{+}^{(1)})]}{[1 + \tan^2(\theta_{+}^{(1)}) + \tan^2(\varphi_{+}^{(1)})]^{1/2}}, \quad \mathbf{z}_{0}^{(1)} = \frac{[1, i \tan(\theta_{0}^{(1)}), i \tan(\varphi_{0}^{(1)})]}{[1 + \tan^2(\theta_{0}^{(1)}) + \tan^2(\varphi_{0}^{(1)})]^{1/2}}, \quad \mathbf{z}_{-}^{(1)} = \frac{[i \tan(\theta_{-}^{(1)}), \tan(\varphi_{-}^{(1)}), 1]}{[1 + \tan^2(\theta_{-}^{(1)}) + \tan^2(\varphi_{-}^{(1)})]^{1/2}}. \quad (53)$$

It is convenient to emphasize that these eigenstates have been calculated with accuracy of terms  $\sim \sigma(g^2)$ ,  $\sim \sigma(\alpha^2)$  and  $\sim \sigma(g\alpha)$ . Here, the pair  $\theta_{+}^{(1)}, \theta_{0}^{(1)}$  parametrizes the ALP-photon oscillations in which photons with positive helicity are involved. Explicitly,

$$\tan(\theta_{+}^{(1)}) = \left. \frac{\phi(k + \varkappa)}{if_{+}(k)} \right|_{\omega=w_{+}^{(1)}} = \frac{gm_*^2 \sqrt{I}}{8\sqrt{2\pi}\varepsilon_{\mathbf{k}+\varkappa}\varkappa_0(\varepsilon_{\mathbf{k}+\varkappa} - \varkappa_0 - \omega_{\mathbf{k}})}, \quad (54)$$

$$\tan(\theta_{0}^{(1)}) = \left. \frac{f_{+}(k)}{i\phi(k + \varkappa)} \right|_{\omega=w_{0}^{(1)}} = \frac{gm_*^2 \pi \sqrt{I}}{2\sqrt{2\pi}\omega_{\mathbf{k}}\varkappa_0(\varepsilon_{\mathbf{k}+\varkappa} - \varkappa_0 - \omega_{\mathbf{k}})}, \quad (55)$$

$$\tan(\theta_{-}^{(1)}) = \left. \frac{\phi(k + \varkappa)}{if_{-}(k + 2\varkappa)} \right|_{\omega=w_{-}^{(1)}} = \frac{gm_*^2 \sqrt{I}}{8\sqrt{2\pi}\varepsilon_{\mathbf{k}+\varkappa}\varkappa_0(\varepsilon_{\mathbf{k}+\varkappa} + \varkappa_0 - \omega_{\mathbf{k}+2\varkappa})}. \quad (56)$$

We stress that  $m_*$  is given in Eq. (40). On the other hand, the expression of  $\varepsilon_{\mathbf{k}+\boldsymbol{\varkappa}}$  can be read off from Eq. (43) and (44). The remaining angles contained in  $\mathbf{z}_\lambda^{(1)}$  describe the mixing between photons with different helicities. They read

$$\tan(\varphi_+^{(1)}) = - \left. \frac{f_-(k+2\boldsymbol{\varkappa})}{f_+(k)} \right|_{\omega=w_+^{(1)}} = \frac{\pi_0}{\omega_{\mathbf{k}+2\boldsymbol{\varkappa}}(\omega_{\mathbf{k}} - \omega_{\mathbf{k}+2\boldsymbol{\varkappa}} + 2\boldsymbol{\varkappa}_0)}, \quad (57)$$

$$\tan(\varphi_0^{(1)}) = - \left. \frac{f_-(k+2\boldsymbol{\varkappa})}{i\phi(k+\boldsymbol{\varkappa})} \right|_{\omega=w_0^{(1)}} = \frac{gm_*^2\pi\sqrt{I}}{2\sqrt{2\pi}\omega_{\mathbf{k}+2\boldsymbol{\varkappa}}\boldsymbol{\varkappa}_0(\omega_{\mathbf{k}} - \omega_{\mathbf{k}+2\boldsymbol{\varkappa}} + 2\boldsymbol{\varkappa}_0)}, \quad (58)$$

$$\tan(\varphi_-^{(1)}) = \left. \frac{f_+(k)}{f_-(k+2\boldsymbol{\varkappa})} \right|_{\omega=w_-^{(1)}} = \frac{\pi_0}{\omega_{\mathbf{k}}(\omega_{\mathbf{k}} - \omega_{\mathbf{k}+2\boldsymbol{\varkappa}} + 2\boldsymbol{\varkappa}_0)}, \quad (59)$$

where the explicit expression of  $\pi_0$  can be found in Eq. (26).

We continue our analysis by Fourier transforming Eq. (52) only in time. Next, we consider the experimental setup in which the incoming probe beam is a linearly polarized plane wave. Upon entering in the region occupied by the external field of the wave, the probe beam is decomposed into its circular-polarized waves [Eq. (29)]. In connection, we suppose that at  $t = 0$  only the incoming beam has a nonvanishing amplitude with  $f_\pm(\mathbf{k}, 0) = a_0$ . Guided by this procedure, one obtains a system of algebraic equations for  $\mathcal{N}_\lambda^{(1)}$ . Its solution allows us to express the flavor-like components in the following form:

$$\begin{aligned} f_+(\mathbf{k}, t) &\simeq a_0 e^{-i\omega_+^{(1)}t} \left\{ 1 - \theta_+^{(1)}\theta_0^{(1)} \left[ 1 - e^{i(\omega_+^{(1)} - \omega_0^{(1)})t} \right] - \varphi_+^{(1)}\varphi_-^{(1)} \left[ 1 - e^{i(\omega_+^{(1)} - \omega_-^{(1)})t} \right] \right\}, \\ \phi(\mathbf{k} + \boldsymbol{\varkappa}, t) &\simeq -ia_0\theta_+^{(1)} e^{-i(\omega_0^{(1)} + \boldsymbol{\varkappa}_0)t} \left[ 1 - e^{i(\omega_0^{(1)} - \omega_+^{(1)})t} \right], \quad f_-(\mathbf{k} + 2\boldsymbol{\varkappa}, t) \simeq a_0\varphi_+^{(1)} e^{-i(\omega_-^{(1)} + 2\boldsymbol{\varkappa}_0)t} \left[ 1 - e^{i(\omega_-^{(1)} - \omega_+^{(1)})t} \right], \end{aligned} \quad (60)$$

where the approximations of weak mixing [ $\theta_\lambda^{(1)}, \varphi_\lambda^{(1)} \ll 1$ ] have been used. The solutions found in this way reveal that the outgoing probe beam contains electromagnetic radiation resulting from the inelastic scattering. These kind of evanescent waves should emerge, in first instance, due to the vacuum polarization effects. Note that Eq. (60) neither depend on  $\theta_-^{(1)}$  nor  $\varphi_0^{(1)}$ . This is because they are associated with higher order processes<sup>5</sup> whose contributions can be ignored.

The determination of the flavor-like fields associated with the second eigenproblem is quite similar to the case previously analyzed. Following the same line of reasoning, we note that the normalized eigenstates of  $\mathcal{G}^{(2)}(k)$  can be found from Eq. (53), provided the replacement  $1 \rightarrow 2$ . The corresponding mixing angles can be obtained from Eqs. (54)-(59) by applying the symmetry transformation that connects both eigenproblems [see below Eq. (32)]. However, in contrast to the previous case, the leading order terms of the flavor-like fields are given by

$$\begin{aligned} f_-(\mathbf{k}, t) &\simeq a_0 e^{-i\omega_-^{(2)}t} \left\{ 1 - \theta_-^{(2)}\theta_0^{(2)} \left[ 1 - e^{i(\omega_-^{(2)} - \omega_0^{(2)})t} \right] - \varphi_-^{(2)}\varphi_+^{(2)} \left[ 1 - e^{i(\omega_-^{(2)} - \omega_+^{(2)})t} \right] \right\}, \\ \phi(\mathbf{k} - \boldsymbol{\varkappa}, t) &\simeq -ia_0\theta_-^{(2)} e^{-i(\omega_0^{(2)} - \boldsymbol{\varkappa}_0)t} \left[ 1 - e^{i(\omega_0^{(2)} - \omega_-^{(2)})t} \right], \quad f_+(\mathbf{k} - 2\boldsymbol{\varkappa}, t) \simeq -a_0\varphi_-^{(2)} e^{-i(\omega_+^{(2)} - 2\boldsymbol{\varkappa}_0)t} \left[ 1 - e^{i(\omega_+^{(2)} - \omega_-^{(2)})t} \right]. \end{aligned} \quad (61)$$

While the angles

$$\theta_-^{(2)} \simeq \left. \frac{\phi(k - \boldsymbol{\varkappa})}{if_-(k)} \right|_{\omega=w_-^{(2)}} = \frac{gm_*^2\sqrt{I}}{8\sqrt{2\pi}\varepsilon_{\mathbf{k}-\boldsymbol{\varkappa}}\boldsymbol{\varkappa}_0(\varepsilon_{\mathbf{k}-\boldsymbol{\varkappa}} + \boldsymbol{\varkappa}_0 - \omega_{\mathbf{k}})}, \quad \theta_0^{(2)} \simeq \left. \frac{f_-(k)}{i\phi(k - \boldsymbol{\varkappa})} \right|_{\omega=w_0^{(2)}} = \frac{gm_*^2\pi\sqrt{I}}{2\sqrt{2\pi}\omega_{\mathbf{k}}\boldsymbol{\varkappa}_0(\varepsilon_{\mathbf{k}-\boldsymbol{\varkappa}} - \boldsymbol{\varkappa}_0 - \omega_{\mathbf{k}})}, \quad (62)$$

describe the respective ALP-photon mixing, the remaining ones are associated with the oscillations between photons with different helicities. These can be approached by

$$\varphi_-^{(2)} \simeq - \left. \frac{f_+(k - \boldsymbol{\varkappa})}{if_-(k)} \right|_{\omega=w_-^{(2)}} = \frac{\pi_0}{\omega_{\mathbf{k}-2\boldsymbol{\varkappa}}(\omega_{\mathbf{k}} - \omega_{\mathbf{k}-2\boldsymbol{\varkappa}} - 2\boldsymbol{\varkappa}_0)}, \quad \varphi_+^{(2)} \simeq \left. \frac{f_-(k)}{if_+(k - 2\boldsymbol{\varkappa})} \right|_{\omega=w_+^{(2)}} = \frac{\pi_0}{\omega_{\mathbf{k}}(\omega_{\mathbf{k}} - \omega_{\mathbf{k}-2\boldsymbol{\varkappa}} - 2\boldsymbol{\varkappa}_0)}. \quad (63)$$

<sup>5</sup>For instance, the oscillations between the Raman-like waves and the axion field.

Observe that when the approximation  $(\omega_{\mathbf{k}} - \varkappa_0)^2 \gg m^2 + m_*^2$  is taking into account, the expression of  $\varepsilon_{\mathbf{k}-\varkappa}$  [Eq. (49)] involved in (62) approaches to  $\varepsilon_{\mathbf{k}-\varkappa} \approx \omega_{\mathbf{k}} - \varkappa_0 + (m^2 + m_*^2)/[2(\omega_{\mathbf{k}} - \varkappa_0)]$ .

In the following, we confine ourselves to the flavor-like electromagnetic waves that are elastically scattered. To this end we re-express the dispersion relations [Eqs. (37) and (47)] in terms of the mixing angles:

$$\omega_+^{(1)}(\mathbf{k}) = \omega_{\mathbf{k}} - \frac{\pi_3}{2\omega_{\mathbf{k}}} - \frac{1}{2} \frac{m^2 - m_*^2}{\omega_{\mathbf{k}} + \varkappa_0} \theta_+^{(1)} \theta_0^{(1)}, \quad \omega_-^{(2)}(\mathbf{k}) = \omega_{\mathbf{k}} - \frac{\pi_3}{2\omega_{\mathbf{k}}} - \frac{1}{2} \frac{m^2 + m_*^2}{\omega_{\mathbf{k}} - \varkappa_0} \theta_-^{(2)} \theta_0^{(2)}. \quad (64)$$

Since we assume that  $\omega_{\mathbf{k}} \gg \frac{\pi_3}{2\omega_{\mathbf{k}}} - \frac{1}{2} \frac{m^2 \mp m_*^2}{\omega_{\mathbf{k}} \pm \varkappa_0} \theta_{\pm}^{(1,2)} \theta_0^{(1,2)}$ , one can write the relevant flavor-like electromagnetic components in the following form

$$f_+(\mathbf{k}, t) \simeq a_0 e^{-i\omega_{\mathbf{k}} t} \left\{ 1 - 2\theta_+^{(1)} \theta_0^{(1)} \sin^2 \left( \frac{1}{4} \frac{m^2 - m_*^2}{\omega_{\mathbf{k}} + \varkappa_0} t \right) - 2\varphi_+^{(1)} \varphi_-^{(1)} \sin^2 \left( \frac{1}{2} \Delta M_+ t \right) + i \left[ \frac{\pi_3}{2\omega_{\mathbf{k}}} t - \varphi_+^{(1)} \varphi_-^{(1)} \sin(\Delta M_+ t) + \frac{\theta_+^{(1)} \theta_0^{(1)}}{2} \frac{m^2 - m_*^2}{\omega_{\mathbf{k}} + \varkappa_0} t - \theta_+^{(1)} \theta_0^{(1)} \sin \left( \frac{1}{2} \frac{m^2 - m_*^2}{\omega_{\mathbf{k}} + \varkappa_0} t \right) \right] \right\}, \quad (65)$$

$$f_-(\mathbf{k}, t) \simeq a_0 e^{-i\omega_{\mathbf{k}} t} \left\{ 1 - 2\theta_-^{(2)} \theta_0^{(2)} \sin^2 \left( \frac{1}{4} \frac{m^2 + m_*^2}{\omega_{\mathbf{k}} - \varkappa_0} t \right) - 2\varphi_+^{(2)} \varphi_-^{(2)} \sin^2 \left( \frac{1}{2} \Delta M_- t \right) + i \left[ \frac{\pi_3}{2\omega_{\mathbf{k}}} t - \varphi_+^{(2)} \varphi_-^{(2)} \sin(\Delta M_- t) + \frac{\theta_-^{(2)} \theta_0^{(2)}}{2} \frac{m^2 + m_*^2}{\omega_{\mathbf{k}} - \varkappa_0} t + \theta_-^{(2)} \theta_0^{(2)} \sin \left( \frac{1}{2} \frac{m^2 + m_*^2}{\omega_{\mathbf{k}} - \varkappa_0} t \right) \right] \right\}, \quad (66)$$

where only the leading terms have been withheld. Note that the following abbreviation  $\Delta M_{\pm} \equiv \omega_{\mathbf{k}} - \omega_{\mathbf{k} \pm 2\varkappa} \pm 2\varkappa_0$  has been used.

### 3.3. Conversion probabilities

The contributions proportional to  $\theta_+^{(1)} \theta_0^{(1)}$ ,  $\theta_-^{(2)} \theta_0^{(2)}$  and  $\varphi_+^{(1,2)} \varphi_-^{(1,2)}$  in Eqs. (65) and (66) are perturbative corrections to the leading order term  $\sim e^{-i\omega_{\mathbf{k}} t}$ . In correspondence, one can express the relevant parts of the photon wave functions of the problem as follows

$$f_{\pm}(\mathbf{k}, t) = \sqrt{\frac{4\pi}{2\omega_{\pm}}} \mathcal{A}_{\pm}(\mathbf{k}, t) e^{-i\omega_{\pm} t}, \quad (67)$$

where the normalization factor  $a_0 = \sqrt{4\pi/2\omega_{\pm}}$  has been chosen. The respective amplitudes of the waves approach to

$$\mathcal{A}_+(\mathbf{k}, t) \approx e^{-i\theta_+^{(1)} \theta_0^{(1)} \sin\left(\frac{1}{2} \frac{m^2 - m_*^2}{\omega_{\mathbf{k}} + \varkappa_0} t\right) - i\varphi_+^{(1)} \varphi_-^{(1)} \sin(\Delta M_+ t) - 2\theta_+^{(1)} \theta_0^{(1)} \sin^2\left(\frac{1}{4} \frac{m^2 - m_*^2}{\omega_{\mathbf{k}} + \varkappa_0} t\right) - 2\varphi_+^{(1)} \varphi_-^{(1)} \sin^2\left(\frac{1}{2} \Delta M_+ t\right)}, \quad (68)$$

$$\mathcal{A}_-(\mathbf{k}, t) \approx e^{-i\theta_-^{(2)} \theta_0^{(2)} \sin\left(\frac{1}{2} \frac{m^2 + m_*^2}{\omega_{\mathbf{k}} - \varkappa_0} t\right) - i\varphi_+^{(2)} \varphi_-^{(2)} \sin(\Delta M_- t) - 2\theta_-^{(2)} \theta_0^{(2)} \sin^2\left(\frac{1}{4} \frac{m^2 + m_*^2}{\omega_{\mathbf{k}} - \varkappa_0} t\right) - 2\varphi_+^{(2)} \varphi_-^{(2)} \sin^2\left(\frac{1}{2} \Delta M_- t\right)}. \quad (69)$$

The substitution of Eqs. (67)-(69) into Eq. (29) allows us to analyze the part of the probe beam which is elastically scattered. The resulting electromagnetic wave involves the effects coming from an ALP, a fact to be exploited in the search of this weakly interacting particle.

Clearly, the square of  $\mathcal{A}_{\pm}(\mathbf{k}, t)$  provides the survival probability for an incoming photon with positive/negative helicity  $\mathcal{P}_{\gamma_{\pm} \rightarrow \gamma_{\pm}}(\mathbf{k}, t) = \mathcal{A}_{\pm}^*(\mathbf{k}, t) \mathcal{A}_{\pm}(\mathbf{k}, t)$ . The resulting expressions are intrinsically associated with the exponentials responsible for the damping of the corresponding electromagnetic waves due to both the photo-production of an ALP and the generation of Raman-like photons. Since the respective exponents are extremely small, the terms proportional to  $\theta_{\pm} \theta_0$  define the photo-production probabilities of an ALP in the field of a strong wave. Explicitly

$$\mathcal{P}_{\gamma_{\pm} \rightarrow \phi_{\pm}} \simeq \frac{g^2 \text{Im}_*^4(\omega_{\mathbf{k}} \pm \varkappa_0)}{2\omega_{\mathbf{k}} \varkappa_0^2 (m^2 \mp m_*^2)^2} \sin^2 \left( \frac{1}{4} \frac{m^2 \mp m_*^2}{\omega_{\mathbf{k}} \pm \varkappa_0} t \right), \quad (70)$$

where the following abbreviations  $\gamma_{\pm} \equiv f_{\pm}(k)$ ,  $\phi_{\pm} \equiv \phi(k \pm \varkappa)$  have been introduced. Note that both probabilities  $\mathcal{P}_{\gamma_{\pm} \rightarrow \phi_{\pm}}$  vanish identically when  $g \rightarrow 0$ . It is worth mentioning that the following limit  $\lim_{t \rightarrow \infty} \mathcal{P}_{\gamma_{\pm} \rightarrow \phi_{\pm}}(t)/t = \mathcal{R}_{\pm}$  provides the

conversion rates in a pure monochromatic plane wave. Considering the relation  $\pi\delta(x) = \lim_{\tau \rightarrow \infty} \sin^2(x\tau)/(x^2\tau)$  we find that

$$\mathcal{R}_{\pm} = \frac{g^2 m_*^4 I \pi}{8 \omega_{\mathbf{k}} \varkappa_0^2} \delta(m^2 \mp m_*^2). \quad (71)$$

Manifestly, Eq. (71) shows that only the resonant process can occur in a monochromatic plane wave, a fact which verifies the statement written above Eq. (50).

The rate  $\mathcal{R}_{\pm}$  coincides with the one obtained from the standard perturbation theory when the involved fields are canonically light-front-quantized [85]. Its singularity at  $m = m_*$  is an outcome of considering an infinity interacting time. This fact motivates us to investigate the realistic case where the field of the wave [Eq. (8)] has a finite pulse length. In such a case it is expected that the Dirac delta in Eq. (71) be smeared out to a smooth function. The formalism developed in this section provides evidences that this certainly takes place.

Now, the persistence probabilities also contain terms proportional to  $\sim \varphi_+^{(1,2)} \varphi_-^{(1,2)}$  which take into account the generation of Raman-like waves. Such terms reproduce the general expression for the probability found in [79]. We combine the respective outcomes to express the total photo-production probability of Raman-like waves as

$$\begin{aligned} \mathcal{P}_{\gamma \rightarrow \gamma'} &= \mathcal{P}_{\omega \rightarrow \omega + 2\varkappa_0} + \mathcal{P}_{\omega \rightarrow \omega - 2\varkappa_0}, \\ \mathcal{P}_{\omega \rightarrow \omega \pm 2\varkappa_0} &= \frac{4\pi_0^2}{\omega_{\mathbf{k}} \omega_{\mathbf{k} \pm 2\varkappa_0}} \frac{\sin^2\left(\frac{1}{2} [(\omega_{\mathbf{k}} - \omega_{\mathbf{k} \pm 2\varkappa_0} \pm 2\varkappa_0] t\right)}{(\omega_{\mathbf{k}} - \omega_{\mathbf{k} \pm 2\varkappa_0} \pm 2\varkappa_0)^2}, \end{aligned} \quad (72)$$

where the expressions for  $\pi_0$  can be found in Eq. (26). We remark that the expression above applies whenever the condition  $k\varkappa \simeq 0$  is fulfilled [see comment below Eq. (38)]. So, it can be used in the case in which both lasers propagate quasi-parallelly, i.e., when  $k\varkappa \approx \omega_{\mathbf{k}} \varkappa_0 \theta^2 / 2 \ll 1$  with  $\theta$  denoting the collision angle [ $\theta \ll 1$ ]. As a consequence, the conversion probability, resulting from the substitution of Eq. (26) into Eq. (72), is given by

$$\mathcal{P}_{\omega \rightarrow \omega \pm 2\varkappa_0} \approx \frac{\alpha^2 m_*^4 \xi^4}{120^2 \pi^2 m_0^4} \left| 1 \pm 2 \frac{\varkappa_0}{\omega_{\mathbf{k}}} \right| \sin^2\left(\frac{m_*^2}{\omega_{\mathbf{k}} \pm 2\varkappa_0} t\right). \quad (73)$$

It is opportune to emphasize that Eq. (73) applies for  $\omega_{\mathbf{k}} > 2\varkappa_0$  or  $2\varkappa_0 > \omega_{\mathbf{k}}$ . In this context the resonant mass approaches to  $m_* \simeq \theta(\omega_{\mathbf{k}} \varkappa_0)^{1/2}$ . Once Eq. (73) is established, one can estimate the number of Raman-like photons generated during the interaction by considering the relation  $\mathcal{N} = \mathcal{N}_0 \mathcal{P}_{\gamma \rightarrow \gamma'}$  where  $\mathcal{N}_0$  denotes the number of incoming probe photons per shot. A positive detection of such inelastic waves would constitute a strong signature of the non-linearity of the quantum vacuum. Unfortunately, the probability associated with this process is extremely small  $\sim \theta^4$ , and even for the forthcoming high-intensity laser facilities, the generation of a single Raman-like photon seems to be extremely difficult to achieve. It is convenient to remark that the production rate of Raman-like waves vanishes identically when both laser waves counterpropagate and the strong one approaches to the strict monochromatic situation [79].

#### 4. Exclusion limits

Hereafter, we ignore the optical effects resulting from the Raman-like waves, and focus on those associated with the axion-photon conversion. In the field of a circularly polarized plane wave, the vacuum behaves as a chiral medium rather than a biaxial crystal [79]. As a consequence, the rotation of the polarization plane and the ellipticity of the outgoing probe beam [Eq. (29) with Eqs. (67)-(69) included] are determined by the relative phase between the propagating modes and the difference between the photon absorption coefficients, respectively. Consequently, the ellipticity of our problem approaches [85]

$$\psi(t) \approx \frac{1}{4} \left| \mathcal{P}_{\gamma_- \rightarrow \phi_-} - \mathcal{P}_{\gamma_+ \rightarrow \phi_+} \right| \quad (74)$$

with  $\mathcal{P}_{\gamma_{\pm} \rightarrow \phi_{\pm}}$  as given in Eq. (70). However, when evaluating  $\psi(t)$ , we have to keep in mind that the experiment must include an external field which approaches our monochromatic model [Eq. (8)]. In practice, the monochromaticity of

the high-intensity laser wave can be implemented by choosing an appropriate experimental setup in which the laser-source emits a pulse with an oscillation period  $\sim \varkappa_0^{-1}$  much smaller than its temporal length  $\tau$ , i.e.  $\varkappa_0\tau \gg 1$ . For  $t = \tau$ , it is expected that the main contribution to the ellipticity comes from the resonant term as it is dictated by Eq. (71):

$$\psi(\tau) \approx \frac{1}{4} \mathcal{P}_{\gamma_+ \rightarrow \phi_+} = \frac{g^2 I m_*^4 (\omega_{\mathbf{k}} + \varkappa_0)}{8 \omega_{\mathbf{k}} \varkappa_0^2 (m^2 - m_*^2)^2} \sin^2 \left( \frac{1}{4} \frac{m^2 - m_*^2}{\omega_{\mathbf{k}} + \varkappa_0} \tau \right), \quad (75)$$

where  $m_*$  is the resonant mass [Eq. (40)]. At this point it is worth mentioning that Eq. (75) applies whenever the condition  $(\omega_{\mathbf{k}} + \varkappa_0)^2 \gg 2\epsilon m_*$  is fulfilled. If  $\epsilon \ll 1$  eV and  $m_* \sim 1$  eV, we can then restrict ourselves to the case in which  $\omega_{\mathbf{k}} > \varkappa_0$  with  $\omega_{\mathbf{k}}, \varkappa_0 \sim 1$  eV, i.e. optical laser waves. Note that  $\psi(\tau)$  is maximized when the trigonometric argument is very small, in which case we find that

$$\psi(\tau) \approx \frac{1}{128} g^2 \frac{I_c}{m_0^2} \frac{m_*^4}{\omega_{\mathbf{k}} (\omega_{\mathbf{k}} + \varkappa_0)} \xi^2 \tau^2. \quad (76)$$

In this expression  $I_c = m_0^4 / (4\pi e^2) \approx 4.6 \times 10^{29}$  W/cm<sup>2</sup> denotes the critical intensity, with  $m_0$  and  $|e|$  the electron mass and absolute charge, respectively. The square of the intensity parameter  $\xi^2 = m_0^2 I / (\varkappa_0^2 I_c)$  is as defined in Eq. (13). So, near resonance, an enhancement of the ellipticity could occur as the product  $\xi\tau$  increases.

The situation is different for the angle  $\vartheta(\tau)$  by which the polarization plane is rotated. Whenever the high-intensity laser wave approaches to our monochromatic model, we find

$$\vartheta(\tau) \approx \frac{1}{2} (v_- - v_+) \omega_{\mathbf{k}} \tau - \frac{g^2 m_*^4 I (\omega_{\mathbf{k}} + \varkappa_0)}{16 \omega_{\mathbf{k}} \varkappa_0^2 (m^2 - m_*^2)} \sin \left( \frac{1}{2} \frac{m^2 - m_*^2}{\omega_{\mathbf{k}} + \varkappa_0} \tau \right). \quad (77)$$

Here  $v_+$  and  $v_-$  are the phase velocities of the corresponding propagating modes [Eq. (51)]. The resulting expression also applies whenever the condition  $\omega_{\mathbf{k}} > \varkappa_0$  is satisfied. Note that the first term in Eq. (77) becomes dominant when the resonance is not reached. On the contrary, when the argument of the trigonometric function is very small, the resonance contribution in Eq. (77) vanishes identically and the rotated angle is simply determined by

$$\vartheta(\tau) \approx \frac{1}{2} v_- \omega_{\mathbf{k}} \tau = \frac{1}{64} g^2 \frac{I_c}{m_0^2} \frac{m_*^2}{\omega_{\mathbf{k}}} \xi^2 \tau. \quad (78)$$

Note that, Eq. (76) exceeds Eq. (78) by a factor  $\sim m_*^2 \tau / (\omega_{\mathbf{k}} + \varkappa_0)$  as  $\tau \rightarrow \infty$ . Therefore, near resonance, the detection of the ellipticity seems to be more feasible than the rotation of the polarization plane. This is the main difference between our laser-based setup and investigations based on dipole magnets, where the opposite is true.

Now, we wish to particularize Eqs. (75)-(78) to the case in which the collision is head-on, i.e.  $\mathbf{k} \cdot \boldsymbol{\varkappa} = -\omega_{\mathbf{k}} \varkappa_0$ . Formally, the monochromaticity of our high-intensity laser wave [Eq. (8)] implies to work in the limit of an infinite pulse length [81]. However, in practice, this is a finite quantity and the monochromaticity is guaranteed—up to certain limit—when the strong wave is characterized by a relatively long pulse, i.e.,  $\tau \gg T$  with  $T = 2\pi \varkappa_0^{-1}$  the oscillating period. The previous condition is satisfied by choosing the envisaged parameters associated with OMEGA EP laser system [82] at Rochester, USA. This system will consist of four beamlines, two of which capable of operating with a pulse-width range of 1 – 100 ps at central wavelength  $\lambda_0 \approx 1053$  nm, i.e.,  $\varkappa_0 \approx 1.17$  eV. For a pulse width  $\tau \approx 1$  ps, the system will produce a power of the order of  $\sim 1$  PW, i.e., 1 kJ of pulse energy in 1 ps. Note that in this setup the product  $\varkappa_0 \tau \sim 10^3 \gg 1$ , which justifies its use in our monochromatic approach. We should also mention that the focal spot of the short-pulse beams is 80% of the energy in a  $\sim 10$   $\mu\text{m}$ -radius spot, producing ultrahigh intensities  $I$  exceeding the value  $2 \times 10^{20}$  W/cm<sup>2</sup> corresponding to  $\xi \gtrsim 10$ . We can suppose, in addition, that the experiment is carried out by coupling out a fraction of the strong wave whose frequency is doubled [ $\omega_{\mathbf{k}} = 2\varkappa_0$ ] and is used as the probe beam. This guarantees the necessary synchronization in the collision and allows us to study a resonant mass  $m_* \approx 3.3$  eV. The exclusion limits are then determined by requiring that no significant signals are detected at certain confidence level neither in the ellipticity [Eq. (75)] nor in the rotation angle [Eq. (77)]. Searches of ALPs in a strong background laser field have not been carried out yet. However, in the optical regime of other laser-based experiments, sensitivities of the order of  $\sim 10^{-10}$  rad have been established [83]. Taking this value as reference, a negative result

in the search of the ellipticity [Eq. (76)] would constrain  $g \lesssim 1.3 \times 10^{-6} \text{ GeV}^{-1}$  near resonance. The resulting upper bound improves by two orders of magnitude the constraints reported in [64, 65] by using the technical specification of the POLARIS system [84]. However, it roughly remains two orders of magnitude greater than the best laboratory constraint [29, 30].

A more stringent upper bound could be achieved by taking into account the envisaged experimental parameters of ELI and XCELS projects. These ultra-high-intensity laser systems are planned to deliver a power of  $\sim 1 \text{ EW}$ , with  $\xi \approx 1.54 \times 10^3$  [ $I \approx 10^{25} \text{ W/cm}^2$ ] and central frequency  $\nu_0 \approx 1.55 \text{ eV}$ . For a temporal extension of  $\tau \approx 15 \text{ fs}$  this would not satisfy the monochromaticity condition as well as the OMEGA EP facility. However, a first estimate may be carried out. In fact, by choosing the optical probe wave as a fraction of the main laser beam with  $\omega_k = 2\nu_0$  and by keeping the geometry of the collision, it is found that the upper bound  $g \lesssim 3.8 \times 10^{-7} \text{ GeV}^{-1}$  applies for a resonant mass  $m_* \approx 4.4 \text{ eV}$ . We emphasize that the outcome of this analysis is of particular importance as it allows us to establish the extent to which the monochromatic model correctly describes the phenomenology in these ultra-short laser pulses, through comparisons with more realistic models. In this context, it is worth mentioning that the order of magnitude of our exclusion limit coincides with the one given in [85] [ $g \lesssim 1.8 \times 10^{-7} \text{ GeV}^{-1}$ ], established by considering the external laser field as a Gaussian pulse.

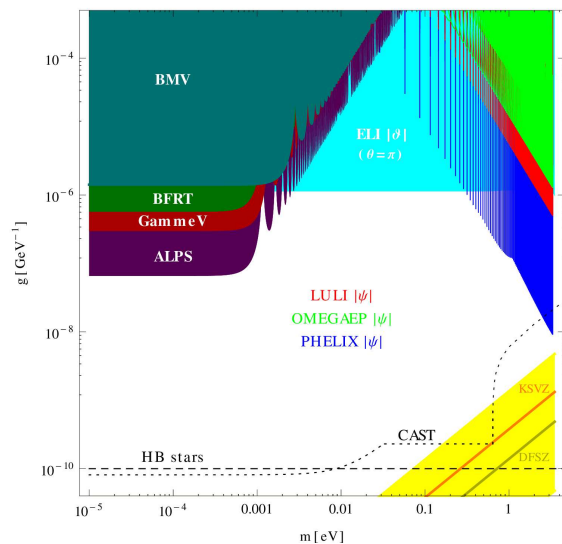


Figure 2: (color online). Constraints for pseudoscalar ALPs of mass  $m$  and coupling constant  $g$  obtained from a plausible polarimetric setup assisted by an intense circularly polarized laser field. Multiple resonant peaks are displayed. They were obtained by varying the collision angle [ $\theta = 1^\circ, 2^\circ, 3^\circ, \dots, 180^\circ$ ] and by considering  $\omega_k = 2\nu_0$ . Also shown are the predictions of the axion models with  $|E/N - 1.95| = 0.07 - 7$  (the notation of this formula is in accordance with Ref. [87]). The constraint resulting from the Horizontal Branch (HB) stars (dashed line) are displayed as well. Further exclusion regions (shaded areas in the upper left corner) provided by different experimental collaborations dealing with the Light Shining Through a Wall mechanism have also been included. The limit resulting from the solar monitoring of a plausible ALP flux [87] is indicated by a dotted line. We remark that the upper bound resulting from such an experiment strongly oscillates in the mass region  $0.4 \text{ eV} \leq m \leq 0.6 \text{ eV}$ . This oscillating pattern has been replaced by the exclusion limit  $g \leq 2.3 \times 10^{-10} \text{ GeV}^{-1}$ , established in [87] at  $2\sigma$  confidence level.

$\nu_0 \approx 1.17 \text{ eV}$ , but its pulse length can reach  $\tau \approx 1.5 \text{ ns}$  for an intensity of  $I \approx 6 \times 10^{14} \text{ W/cm}^2$  [ $\xi \approx 2 \times 10^{-2}$ ]. For comparison, the prediction resulting from the hadronic models of Dine-Fischler-Srednicki-Zhitnitskii (DFSZ) [90, 91]

Eq. (76) shows that a laser pulse with a moderate intensity but with a large pulse length can also be a sensitive probe for pseudoscalar ALPs. We investigate this situation by choosing a set of parameters associated with the Petawatt High-Energy Laser for heavy Ion eXperiments (PHELIX) [86], currently under operation in Darmstadt, Germany. In the nanosecond frontend, PHELIX operates with an infrared wavelength  $\lambda_0 \approx 1053 \text{ nm}$  [ $\nu_0 \approx 1.17 \text{ eV}$ ] and can reach a maximum intensity  $I \approx 10^{16} \text{ W/cm}^2$ , corresponding to  $\xi \approx 6.4 \times 10^{-2}$  in a pulse length  $\tau \approx 20 \text{ ns}$ . This large value of  $\tau$  compensates the relative smallness of  $\xi$ , making the product  $\xi\tau \sim 10^4 \text{ eV}^{-1}$  three orders of magnitude greater than the value resulting from ELI. As for the previous cases, we suppose that the probe beam is an optical laser obtained by coupling out a fraction of the strong laser whose frequency is shifted to  $\omega_k = 2\nu_0 = 2.34 \text{ eV}$  afterwards. By taking a sensitivity level of the order of  $\sim 10^{-10} \text{ rad}$  we find that the upper limit  $g \lesssim 9.1 \times 10^{-9} \text{ GeV}^{-1}$  applies at  $m_* \approx 3.3 \text{ eV}$ .

Our exclusion regions are given in Fig. 2. The outcomes in the upper right corner (blue, green and red) were derived by considering an optical experiment designed to detect a change in the ellipticity. Clearly, the figure shows how the parameter space to be excluded in the  $(g, m)$ -plane increases as different collision angles are chosen [ $\theta = 1^\circ, 2^\circ, 3^\circ, \dots, 180^\circ$ ]. According to Eq. (40) and (75), each angle determines a resonant mass at which the signal is maximized. A set of different resonant peaks translates into an exclusion comb which depends on the strong field source. The upper limit for the specification of the long high-energy pulse of 400 J at the Laboratoire pour l'Utilisation des Lasers Intenses (LULI) [89]—currently in operation at Palaiseau, France—can be seen as well. Similarly to OMEGAEP and PHELIX, the nanosecond facility at LULI(2000) system operates with a central frequency

and Kim-Shifman-Vainshtein-Zakharov (KSVZ) [92, 93] axions have been included. Furthermore, the upper bound from the search for solar axions [87] is indicated by a dashed line.

Summing up, Fig. 2 shows that high-precision polarimetric experiments assisted by the field of a high-intensity laser wave could provide a sensitive probe for pseudoscalar ALPs in region of masses for which a laboratory setup based on dipole magnets provides less stringent limits. As is clear from the plot, our upper bounds are excluded by the constraint resulting from considerations of stellar energy loss due to the axion production in the horizontal branch (HB) stars [88]. However, this kind of constraint must be considered with certain care because there are macroscopic quantities such as temperature and density of the star, whose inclusions can attenuate the limit significantly [6, 94]. This renders well-controlled laboratory searches of ALPs –as the present proposal and the ones dealing with Light Shining Through a Wall setups–crucially important to complement astro-cosmological studies.

## 5. Summary and outlook

In this article, the mixing of photon with an ALP mediated by a strong circularly polarized monochromatic plane wave has been analyzed. The effects resulting from the interaction between a small-amplitude electromagnetic wave and the vacuum polarized by the field of a strong wave were also considered. In correspondence, the low energy behavior of the polarization tensor in the field of a plane wave of arbitrary shape was determined. We have seen that the specific shape of the external wave makes the conversion processes conceptually more complex than in the case where the mixing is assisted by dipole magnets. However, the inherent simplifications of the monochromatic paradigm compared to waves modulated by particular profiles, allows some particular aspects of the ALP-photon oscillations to be established in a concise way.

A detailed perturbative treatment has been implemented for determining the flavor-like fields as well as the relevant dispersion relations. It was found that, in a circularly polarized monochromatic plane wave and at energies below the scale specified by the electron mass, the pure QED vacuum behaves as a nonbirefringent medium. The incorporation of ALP-photon coupling induces a tiny birefringence and dichroism in the vacuum. The corresponding expressions for the ellipticity and the angular rotation of the polarization plane were used to impose exclusion limits on the ALPs attributes. We have also shown that the most stringent constraints on the coupling constant are in the vicinity of resonant masses which depend on the frequency of both laser fields.

While our research does not cover all plausible experimental setups, the general expressions obtained in Sec. 2 certainly apply to other external configurations of laser fields as well. As a consequence, they can be used in cases where the strong plane wave is, for instance, a bichromatic wave or a Gaussian pulse. Both problems are expected to be more cumbersome and procedures other than the one used in this work, may be required. Besides, the analysis in such field configurations might reveal whether the generation of Raman-like waves is favored when both lasers counterpropagate. If so, we will have at our disposal another mechanism for probing the nonlinear behavior of the quantum vacuum. We plan to present detailed studies of these problems in forthcoming publications.

## Acknowledgments

I am very grateful to A. Di Piazza, C. Müller and B. Döbrich, for helpful discussions. I would also like to extend my gratitude to John Farmer and C. Müller for their critical reading and valuable comments on the manuscript.

## References

- [1] R. D. Peccei and H. R. Quinn. *Phys. Rev. Lett.* **38**, 1440 (1977).
- [2] F. Wilczek. *Phys. Rev. Lett.* **40**, 279 (1978).
- [3] S. Weinberg. *Phys. Rev. Lett.* **40**, 223 (1978).
- [4] E. Witten. *Phys. Lett. B* **149**, 351 (1984).
- [5] O. Lebedev and S. Ramos Sanchez. *Phys. Lett. B* **684**, 48 (2010); [arXiv:0912.0477 [hep-ph]].
- [6] H. Gies. *J. Phys. A* **41**, 164039 (2008); [arXiv:0711.1337 [hep-ph]].
- [7] C. Biggio, E. Masso and J. Redondo. *Phys. Rev. D* **79**, 015012 (2009); [arXiv:hep-ph/0604062].
- [8] E. Gabrielli, K. Huitu and S. Roy. *Phys. Rev. D* **74**, 073002 (2006); [arXiv:hep-ph/0604143].
- [9] L. D. Duffy and K. van Bibber. *New J. Phys.* **11**, 105008 (2009); [arXiv:0904.3346 [hep-ph]].
- [10] P. Sikivie. *Int. J. Mod. Phys. A* **25**, 554 (2010); [arXiv:0909.0949 [hep-ph]].
- [11] G. G. Raffelt. *J. Phys. A* **40**, 6607 (2007); [arXiv:hep-ph/0611118].



- [12] H. Baer, A. D. Box and H. Summy, JHEP **1010**, 023 (2010); [arXiv:1005.2215 [hep-ph]].
- [13] P. Sikivie, Phys. Rev. Lett. **51**, 1415 (1983).
- [14] P. Sikivie, Phys. Rev. D. **32**, 2988 (1985).
- [15] L. Maiani, R. Petronzio and E. Zavattini, Phys. Lett. B **175**, 359 (1986).
- [16] G. Raffelt and L. Stodolsky, Phys. Rev. D **37**, 1237 (1988).
- [17] W. Dittrich and H. Gies, “*Probing the quantum vacuum.*” Springer, Heidelberg, (2000).
- [18] S. L. Adler, Ann. Phys. **67**, 599 (1971);
- [19] A. E. Shabad, Ann. Phys. **90**, 166 (1975).
- [20] A. E. Shabad, Sov. Phys. JETP **98**, 186 (2004).
- [21] R. Cameron *et al.* Phys. Rev. D **47**, 3707 (1993);
- [22] E. Zavattini *et al.* [PVLAS Collaboration], Phys. Rev. D **77**, 032006 (2008); [arXiv:0706.3419 [hep-ex]].
- [23] R. Battesti *et al.* Eur. Phys. J. D **46**, 323 (2008).
- [24] S. J. Chen, H. H. Mei and W. T. Ni, Mod. Phys. Lett. A **22**, 2815 (2007); [arXiv:hep-ex/0611050].
- [25] K. Van Bibber, N. R. Dagdeviren, S. E. Koonin, A. Kerman and H. N. Nelson, Phys. Rev. Lett. **59**, 759 (1987).
- [26] S. L. Adler, J. Gamboa, F. Mendez and J. Lopez-Sarrion, Ann. Phys. **323**, 2851 (2008); [arXiv:0801.4739 [hep-ph]].
- [27] P. Arias, J. Jaeckel and A. Ringwald, Phys. Rev. D **82**, 115018 (2010); [arXiv:1009.4875 [hep-ph]].
- [28] J. Redondo and A. Ringwald, Contemp. Phys. **52**, 211 (2011); [arXiv:1011.3741 [hep-ph]].
- [29] K. Ehret *et al.* [ALPS collaboration] Phys. Lett. B **689**, 149 (2010); [arXiv:1004.1313 [hep-ex]].
- [30] K. Ehret *et al.* [ALPS collaboration], Nucl. Instrum. Meth. A **612**, 83 (2009); [arXiv:0905.4159 [physics.ins-det]].
- [31] A. S. Chou *et al.* [GammeV (T-969) Collaboration], Phys. Rev. Lett. **100**, 080402 (2008); [arXiv:0710.3783 [hep-ex]].
- [32] J. H. Steffen and A. Upadhye, Mod. Phys. Lett. A **24**, 2053 (2009); [arXiv:0908.1529 [hep-ex]].
- [33] A. Afanasev *et al.* Phys. Rev. Lett. **101**, 120401 (2008); [arXiv:0806.2631 [hep-ex]].
- [34] P. Pagnat *et al.* [OSQAR Collaboration], Phys. Rev. D **78**, 092003 (2008); [arXiv:0712.3362 [hep-ex]].
- [35] C. Robilliard *et al.* Phys. Rev. Lett. **99**, 190403 (2007); [arXiv:0707.1296 [hep-ex]].
- [36] M. Fouche *et al.* Phys. Rev. D. **78**, 032013 (2008); [arXiv:0808.2800 [hep-ex]].
- [37] L. B. Okun, Sov. Phys. JETP **56**, 502 (1982); [Zh. Eksp. Teor. Fiz. **83** (1982) 892].
- [38] E. Masso and J. Redondo, Phys. Rev. Lett. **97**, 151802 (2006); [arXiv:hep-ph/0606163].
- [39] M. Ahlers, H. Gies, J. Jaeckel, J. Redondo and A. Ringwald, Phys. Rev. D. **76**, 115005 (2007); [arXiv:0706.2836 [hep-ph]].
- [40] M. Ahlers, H. Gies, J. Jaeckel, J. Redondo, and A. Ringwald, Phys. Rev. D. **77**, 095001 (2008); [arXiv:0711.4991 [hep-ph]].
- [41] M. Goodsell, J. Jaeckel, J. Redondo and A. Ringwald, JHEP **0911**, 027 (2009); [arXiv:0909.0515 [hep-ph]].
- [42] E. Dudas, Y. Mambrini, S. Pokorski and A. Romagnoni, JHEP **1210**, 123 (2012); [arXiv:1205.1520 [hep-ph]].
- [43] B. Holdom, Phys. Lett. B **166**, 196 (1986).
- [44] H. Gies, J. Jaeckel and A. Ringwald, Phys. Rev. Lett. **97**, 140402 (2006); [arXiv:hep-ph/0607118].
- [45] J. Jaeckel, Phys. Rev. Lett. **103**, 080402 (2009); [arXiv:0904.1547 [hep-ph]].
- [46] B. Döbrich, H. Gies, N. Neitz and F. Karbstein, Phys. Rev. Lett. **109**, 131802 (2012); [arXiv:1203.2533 [hep-ph]].
- [47] B. Döbrich, H. Gies, N. Neitz and F. Karbstein, Phys. Rev. D **87**, 025022 (2013); [arXiv:1203.4986 [hep-ph]].
- [48] See: <http://www.extreme-light-infrastructure.eu>
- [49] See: <http://www.xcels.iapras.ru/>
- [50] T. Heinzl and O. Schroeder, J. Phys. A **39**, 11623 (2006); [arXiv:hep-th/0605130].
- [51] T. Heinzl, B. Leifeld, K. U. Amthor, H. Schwoerer, R. Sauerbrey and A. Wipf, Opt. Comm. **267**, 318 (2006).
- [52] A. Di Piazza, A. I. Milstein and C. H. Keitel, Phys. Rev. A. **76**, 032103 (2007); arXiv:0704.0695 [hep-ph].
- [53] A. Di Piazza, K. Z. Hatsagortsyan and C. H. Keitel, Phys. Rev. Lett. **97**, 083603 (2006); [arXiv:hep-ph/0602039].
- [54] Ben King, A. Di Piazza and C. H. Keitel, Nature **4**, 92 (2010).
- [55] Ben King, A. Di Piazza and C. H. Keitel, Phys. Rev. A. **82**, 032114 (2010).
- [56] D. Tommasini and H. Michinel, Phys. Rev. A. **82**, 011803 (2010); [arXiv:1003.5932 [hep-ph]].
- [57] K. Hatsagortsyan and G. Y. Kryuchkyan, Phys. Rev. Lett. **107**, 053604 (2011).
- [58] H. Gies, F. Karbstein and N. Seegert, New J. Phys. **15** (2013) 083002 [arXiv:1305.2320 [hep-ph]].
- [59] F. Hebenstreit, R. Alkofer, G. V. Dunne and H. Gies, Phys. Rev. Lett. **102**, 150404 (2009); [arXiv:0901.2631 [hep-ph]].
- [60] M. Ruf, G. R. Mocken, C. Müller, K. Z. Hatsagortsyan and C. H. Keitel, Phys. Rev. Lett **102**, 080402 (2009).
- [61] G. R. Mocken, M. Ruf, C. Müller and C. H. Keitel, Phys. Rev. A **81**, 022122 (2010).
- [62] J. T. Mendonça, Eurphys. Lett. **79**, 21001 (2007).
- [63] H. Gies, Eur. Phys. J. D **55**, 311 (2009); [arXiv:0812.0668 [hep-ph]].
- [64] B. Döbrich and H. Gies, JHEP **1010**, 022 (2010); [arXiv:1006.5579 [hep-ph]].
- [65] B. Döbrich and H. Gies, “*High-Intensity Probes of Axion-Like Particles,*” Contributed to 6th Patras Workshop on Axions, WIMPs and WISPs, Zurich, Switzerland, 5-9 Jul 2010. [arXiv:1010.6161 [hep-ph]].
- [66] W. Heisenberg and H. Euler, Z. Phys. **98**, 714 (1936).
- [67] J. Schwinger, Phys. Rev. **82**, 664, (1951).
- [68] F. J. Dyson, Phys. Rev., **75**, 1736, 1949.
- [69] J. S. Schwinger, Proc. Nat. Acad. Sci., **37**, 452-455, 1951.
- [70] J. S. Schwinger, Proc. Nat. Acad. Sci., **37**, 455-459, 1951.
- [71] R. Alkofer and L. von Smekal, Phys. Rept., **353**, 281, 2001; [arXiv:hep-ph/0007355].
- [72] E. S. Fradkin in Proceedings (Trudy) of the P. N. Lebedev Physics Institute, Vol. **29**, (Consultants Bureau, New York, 1967).
- [73] A. E. Shabad and V. V. Usov, Phys. Rev. D **83**, 105006 (2011); [arXiv:1101.2343 [hep-th]].
- [74] S. Villalba-Chavez and A. E. Shabad, Phys. Rev. D **86**, 105040 (2012); arXiv:1206.4491 [hep-th].
- [75] I. A. Batalin and A. E. Shabad, Zh. Eksp. Teo. Fiz **60**, 894 (1971). [Sov. Phys. JETP **33**, 483 (1971)].

- [76] V. N. Baier, A. I. Mil'shtein and V. M. Strakhovenko. Zh. Eksp. Teo. Fiz. **69**, 1893 (1975); [Sov. Phys. JETP **42**, 961 (1976)].
- [77] W. Becker and H. Mitter, J. Phys. A **8**, 1638 (1975).
- [78] S. Villalba-Chavez and C. Müller. Phys. Lett. B, **718**, 992, 2013; arXiv:1208.3595 [hep-ph].
- [79] S. Villalba-Chavez and C. Müller, Annals Phys. **339**, 460 (2013); arXiv:1306.6456 [hep-ph].
- [80] T. K. Kuo and J. T. Pantaleone. Rev. Mod. Phys. **61**, 937 (1989).
- [81] J. D. Jackson, *Classical electrodynamics*, John Wiley, New York, (1975).
- [82] See: <http://www.lle.rochester.edu>
- [83] K. Muroo et al., J. Opt. Soc. Am. B **20**, 2249 (2003).
- [84] M. Hornung *et al.* Appl. Phys. B **101**, 93 (2010).
- [85] S. Villalba-Chavez and A. Di Piazza, JHEP. **1311**, 136 (2013); arXiv:1307.7935 [hep-ph].
- [86] see: [https://www.gsi.de/en/start/research/forschungsgebiete\\_und\\_experimente/appa\\_pni\\_gesundheit/plasma\\_physicsphelix/phelix.htm](https://www.gsi.de/en/start/research/forschungsgebiete_und_experimente/appa_pni_gesundheit/plasma_physicsphelix/phelix.htm)
- [87] M. Arik *et al.*, Phys. Rev. Lett. **107**, (2011) 261302.
- [88] G. G. Raffelt, Lect. Notes Phys. **741**, 51 (2008).
- [89] C. Labaune *et al.*, Nat. Commun. **4**, 2506 (2013).
- [90] M. Dine, W. Fischler and M. Srednicki, Phys. Lett. B **104**, 199 (1981).
- [91] A. R. Zhitnitskii, Yad. Fiz **31**, 497 (1980); A. R. Zhitnitskii, Sov. J. Nucl. Phys. **31**, 260 (1980) (translation).
- [92] J. E. Kim, Phys. Rev. Lett. **43**, 103 (1979).
- [93] M. A. Shifman, A. I. Vainshtein, V. I. Zakharov, Nucl. Phys. B **166**, 493 (1980).
- [94] J. Jaeckel, E. Masso, J. Redondo, A. Ringwald, and F. Takahashi, Phys. Rev. D **75**, 013004 (2007).